

Supporting Information

How the Conformations of an Internal Junction Contribute to Fold an RNA Domain

Yen-Lin Chen[†], Julie L. Sutton[†], and Lois Pollack*

School of Applied and Engineering Physics

Cornell University

Ithaca, NY 14853

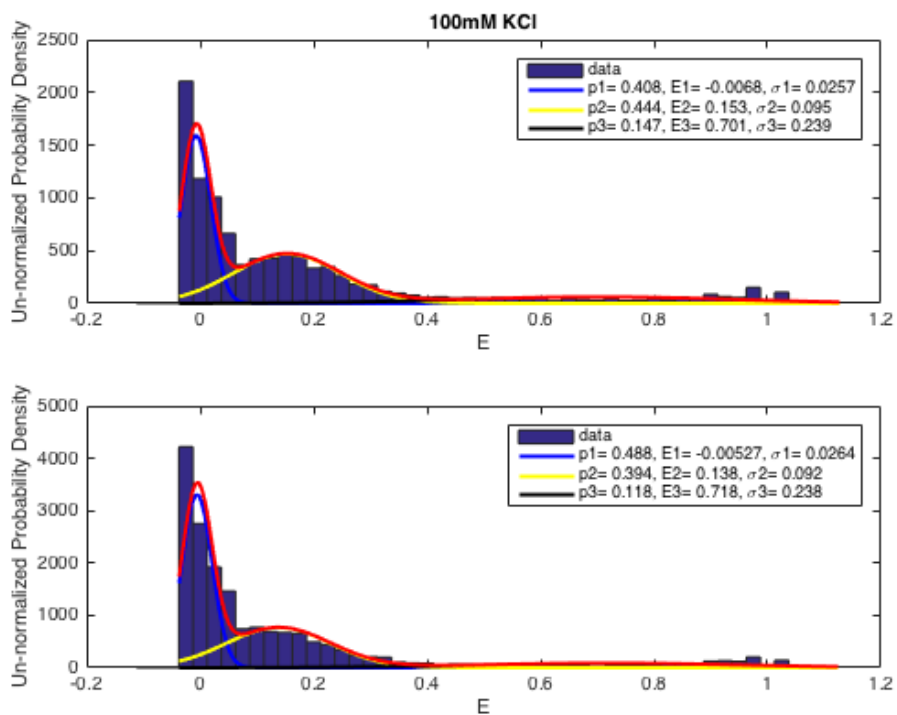
[†] Equal contributions

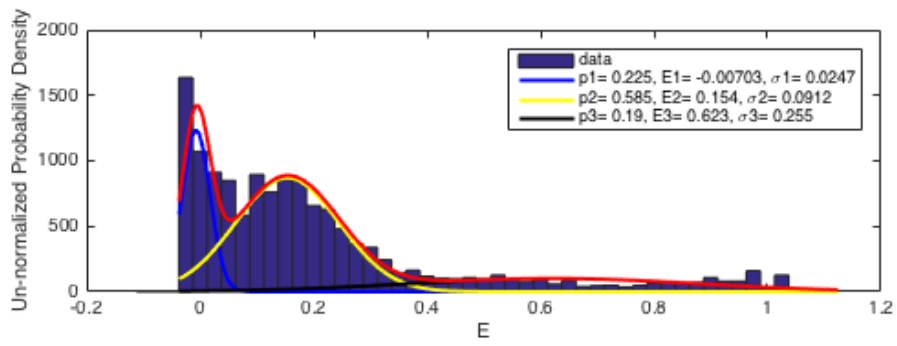
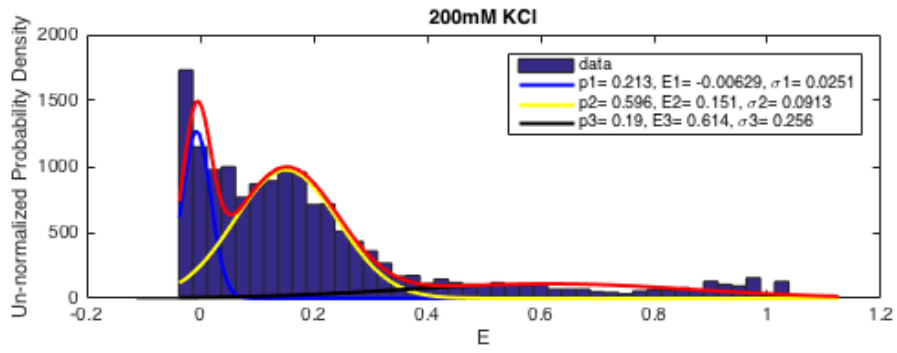
*corresponding author, email: lp26@cornell.edu, phone: 607-255-8695

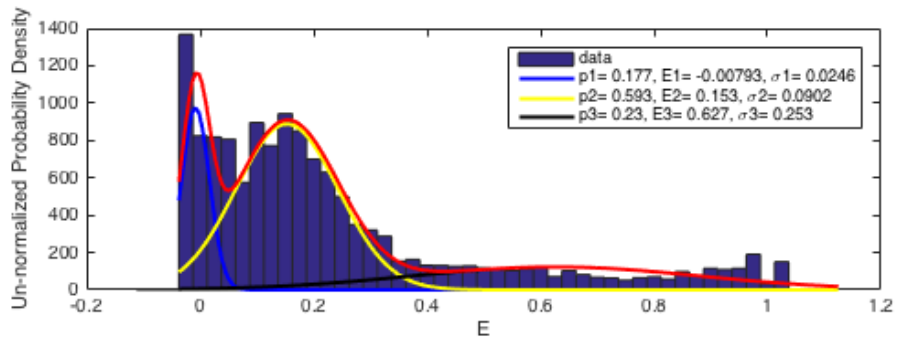
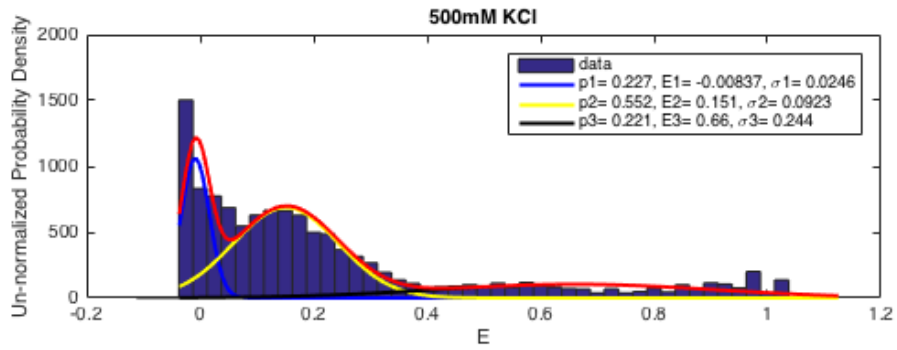
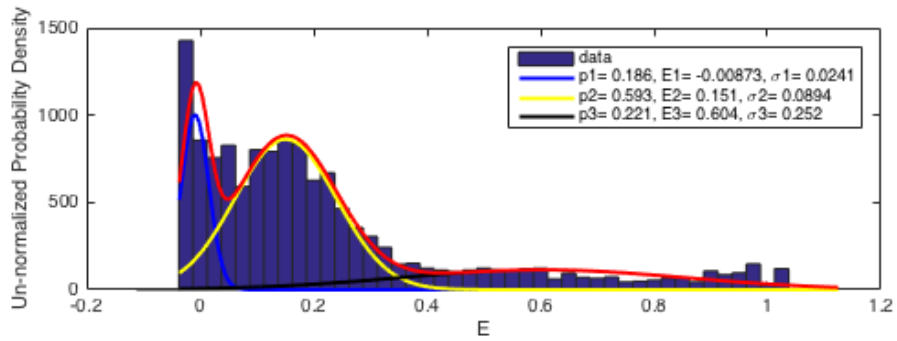
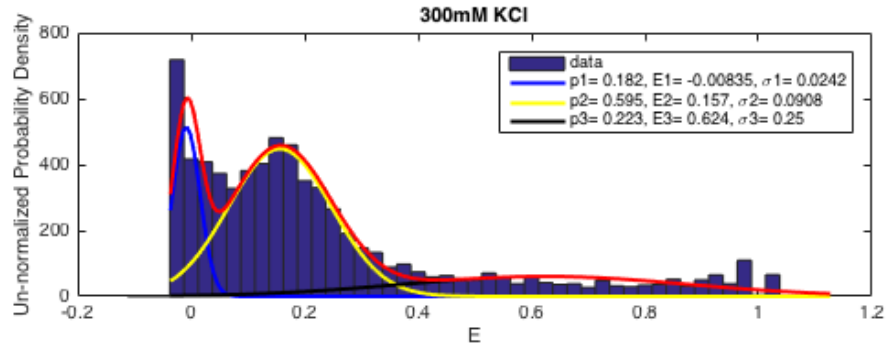
FRET Histograms and E_{FRET} Data

The following figures show the raw FRET data for conditions described in the text. Because the figures contain many panels, the caption is given at the start (top) of each series.

Figure S1 (below). FRET Histograms for H-JU₄U₅-H, D1-A (end labeled) in KCl solutions.







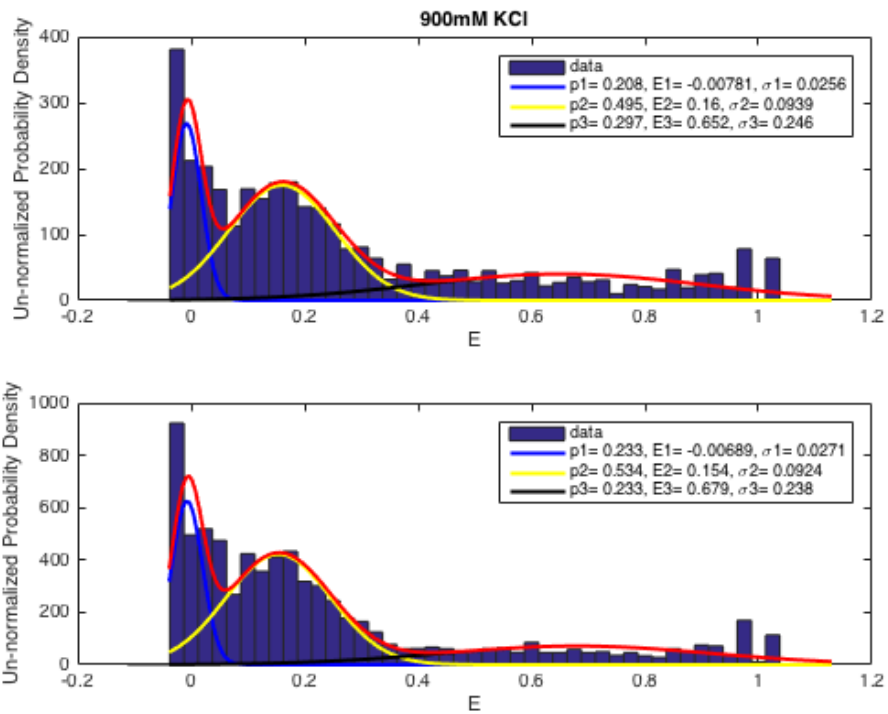
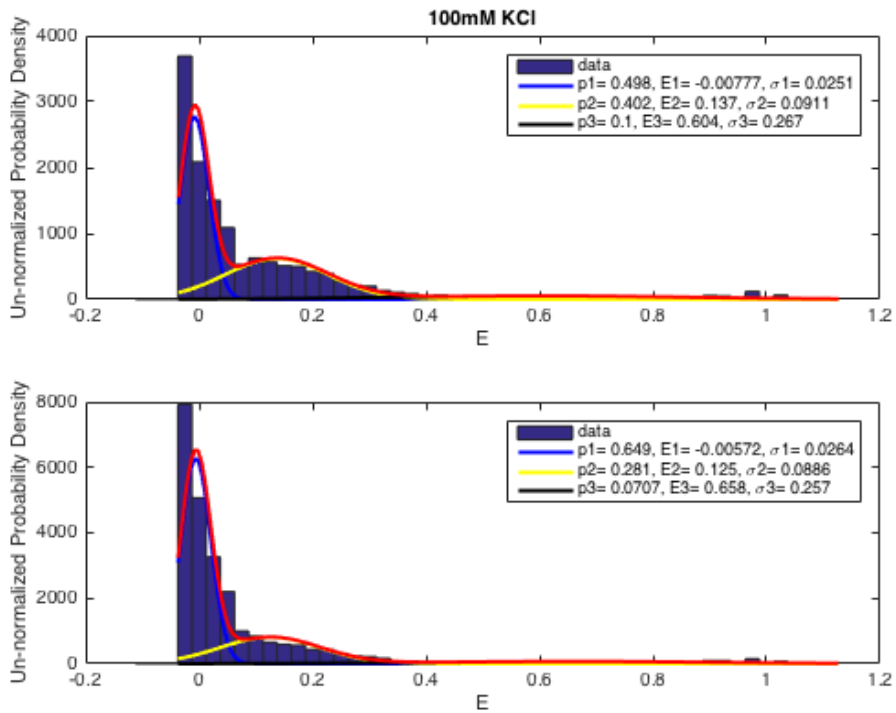
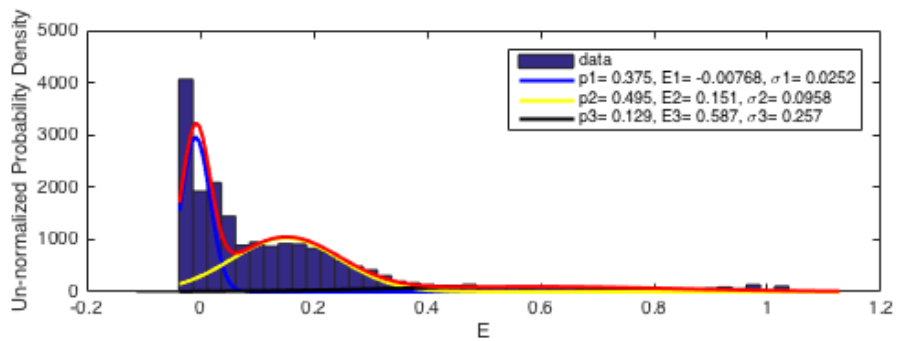
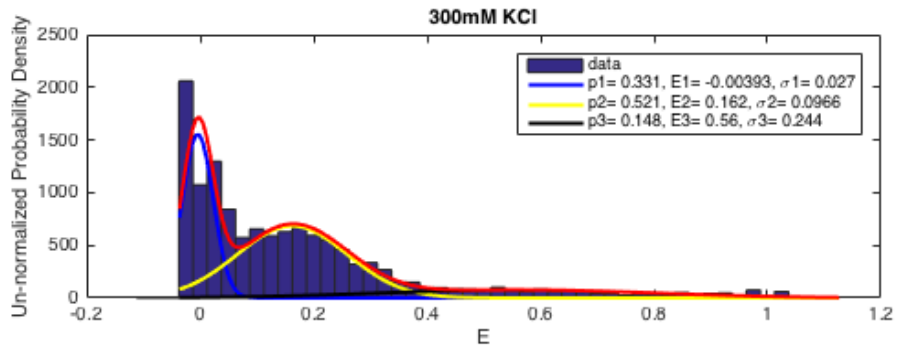
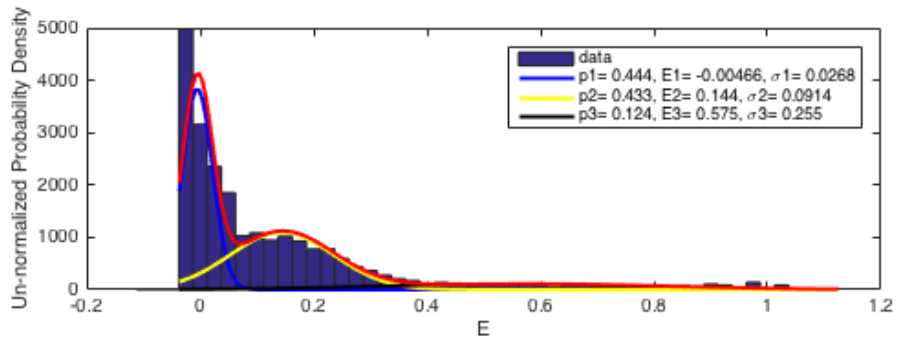
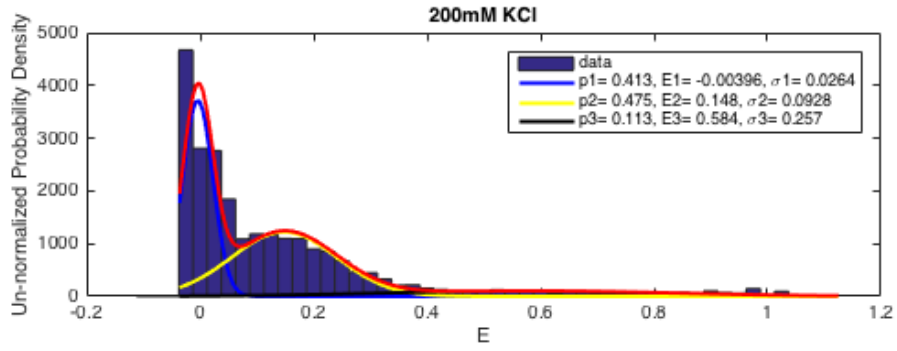


Figure S2 (below). FRET Histograms for H-J5/5a-H, D1-A (end labeled) in KCl solutions.





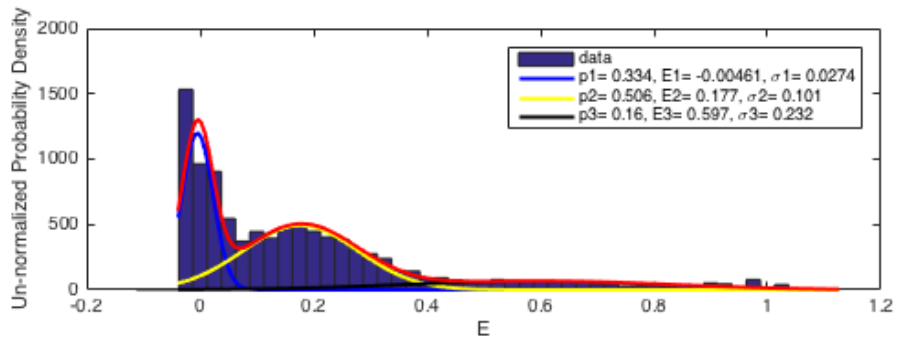
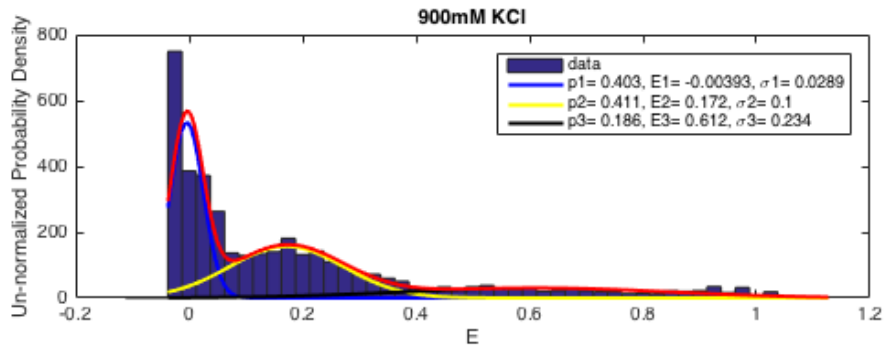
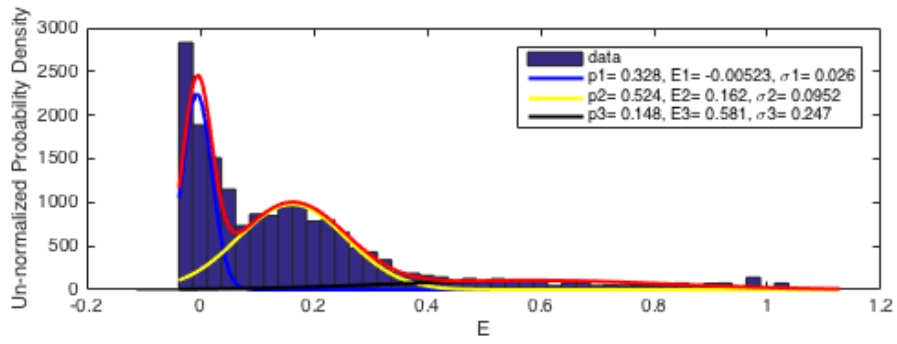
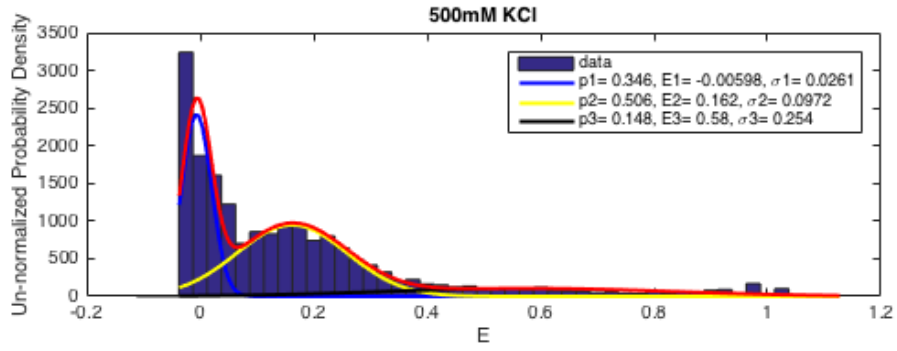
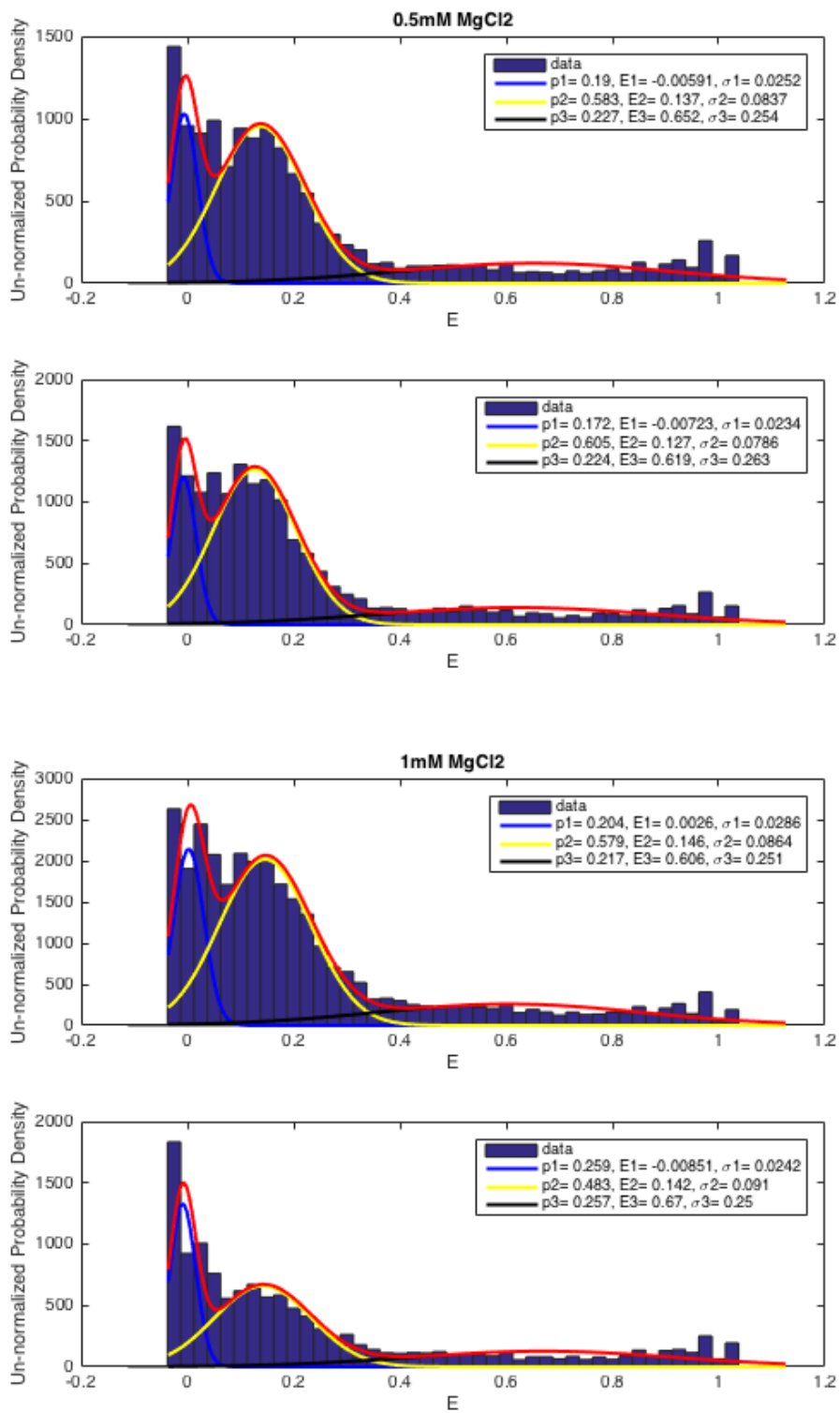
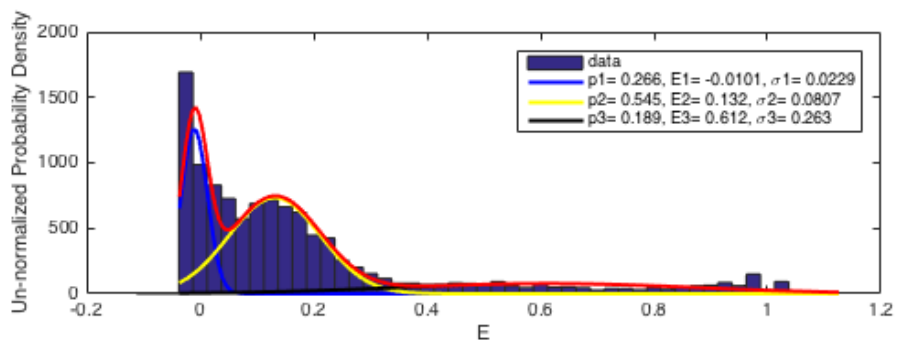
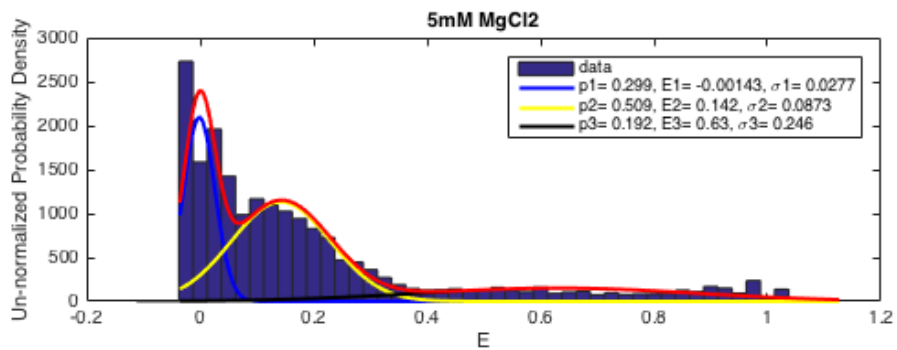
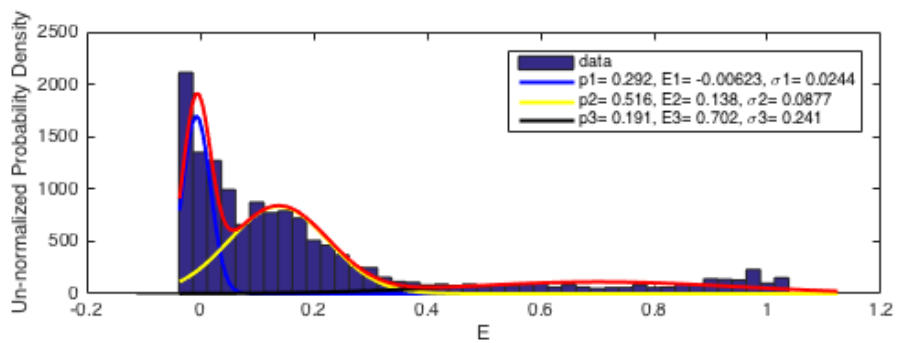
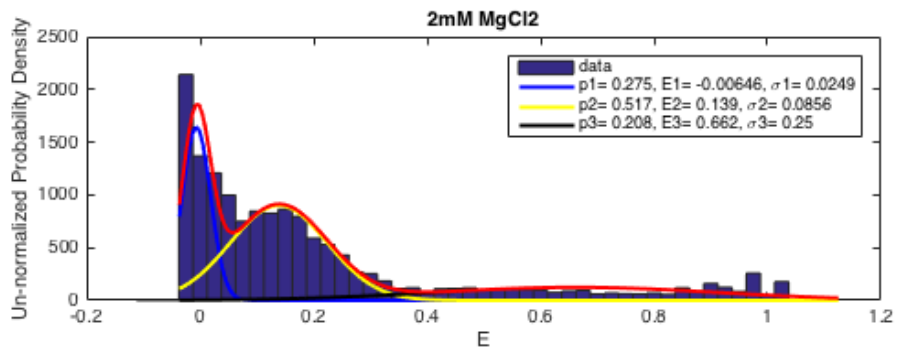
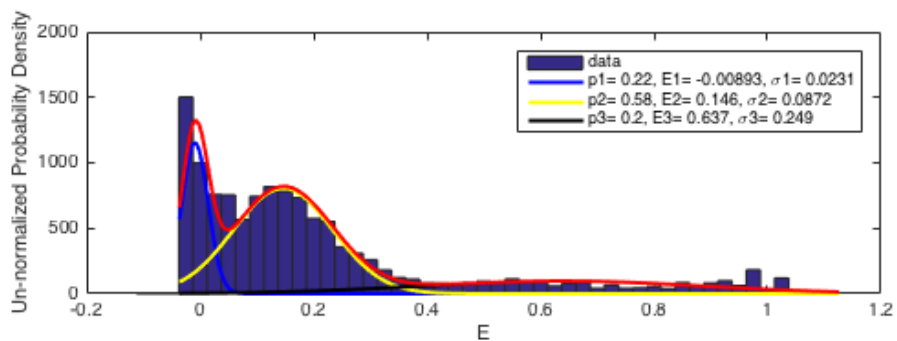
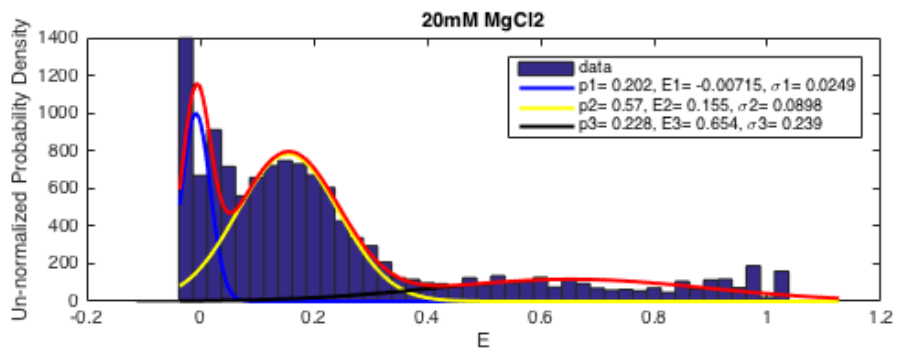
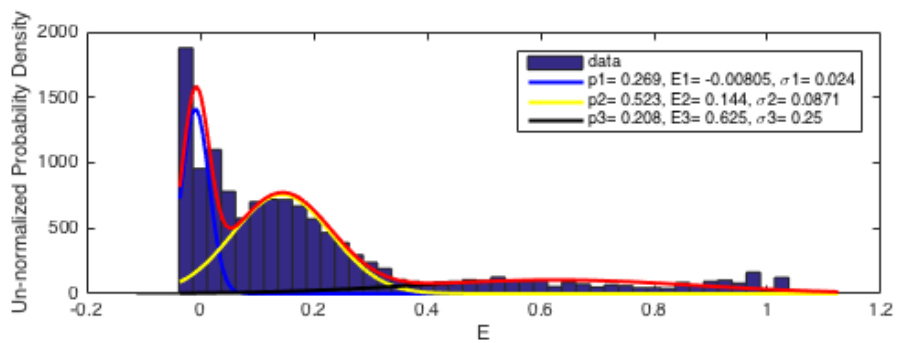
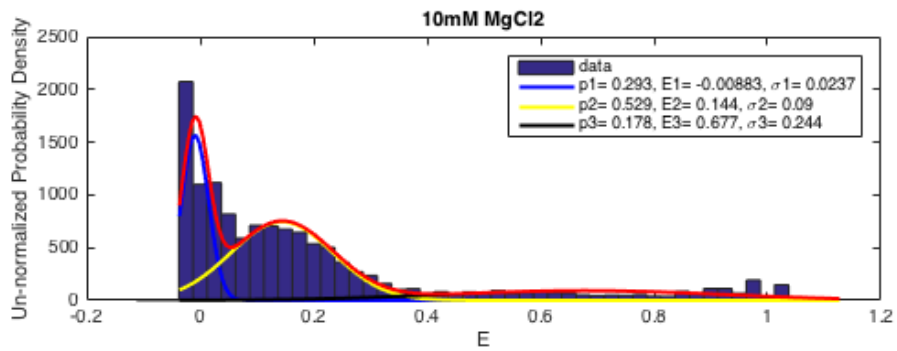


Figure S3 (below). FRET Histograms for H-JU₄U₅-H, D1-A (end labeled) in MgCl₂ solutions.







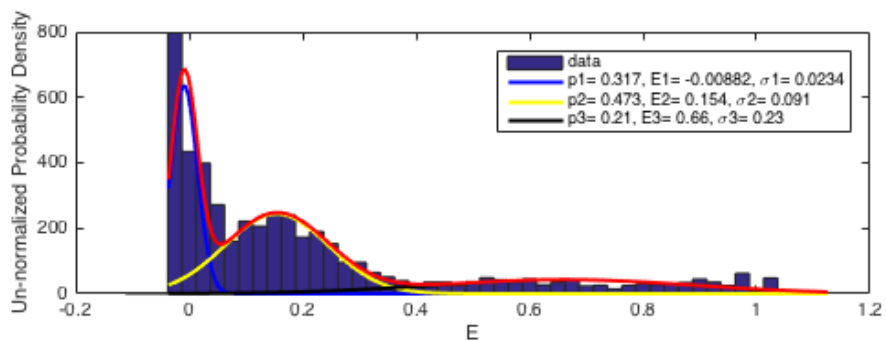
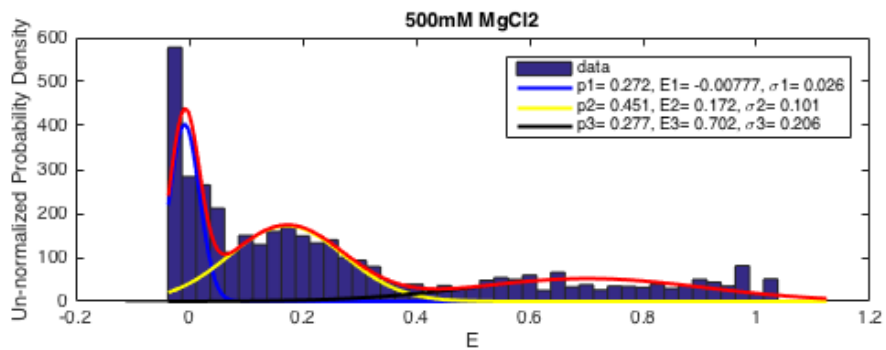
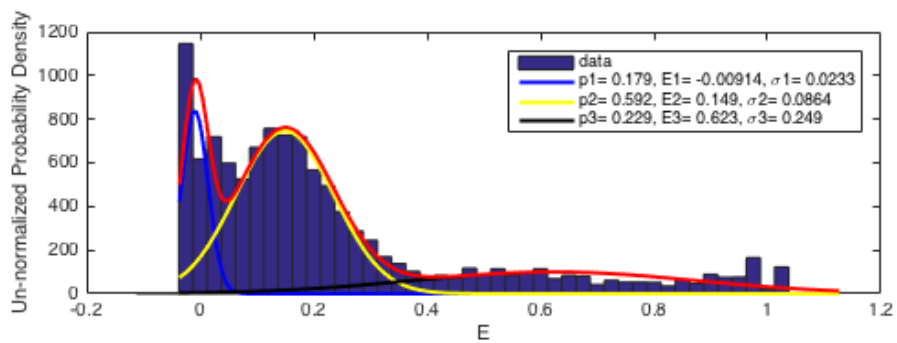
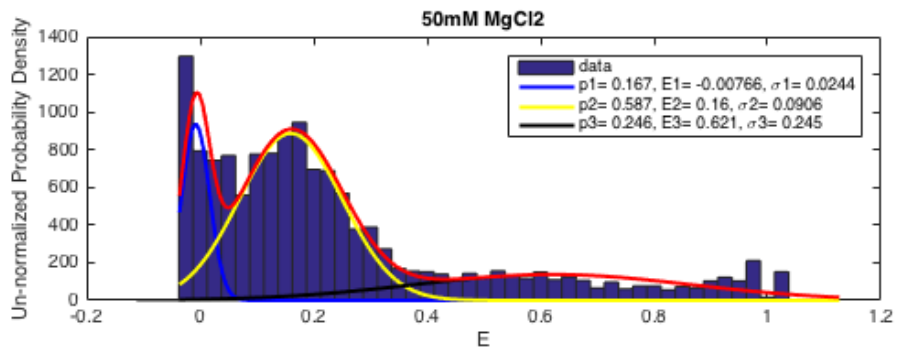
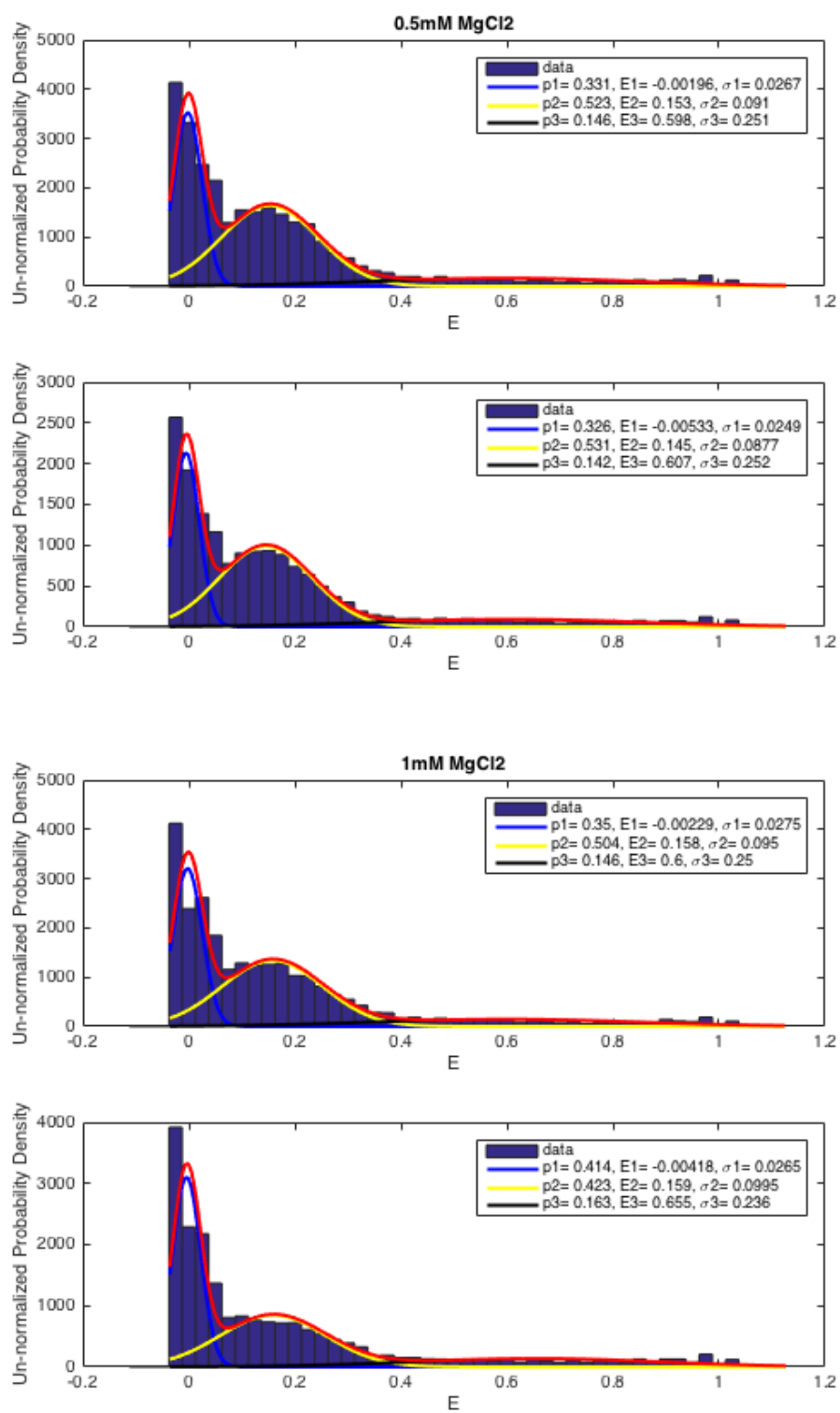
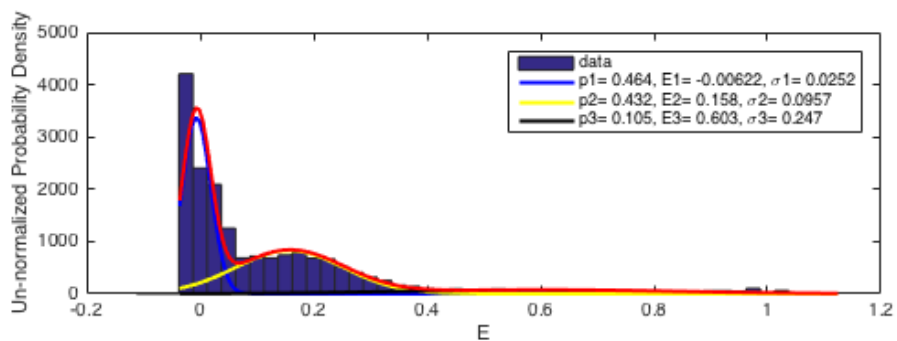
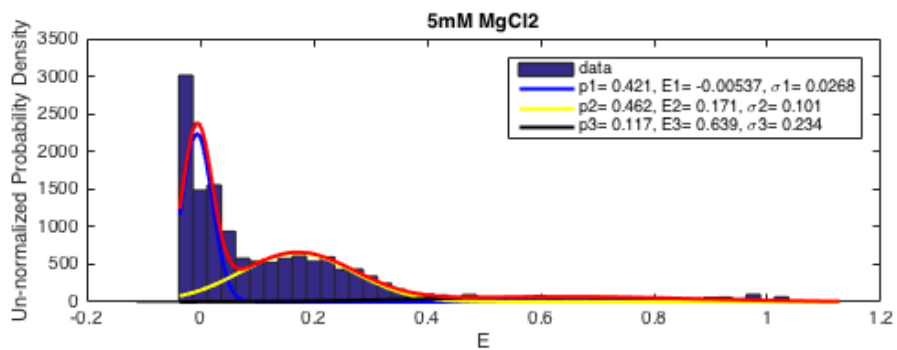
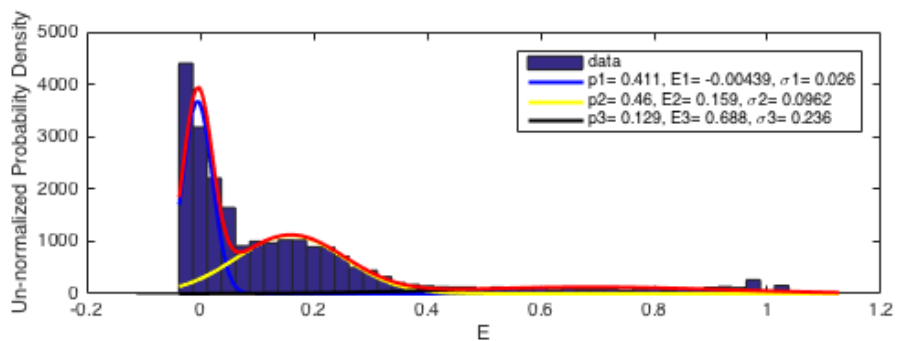
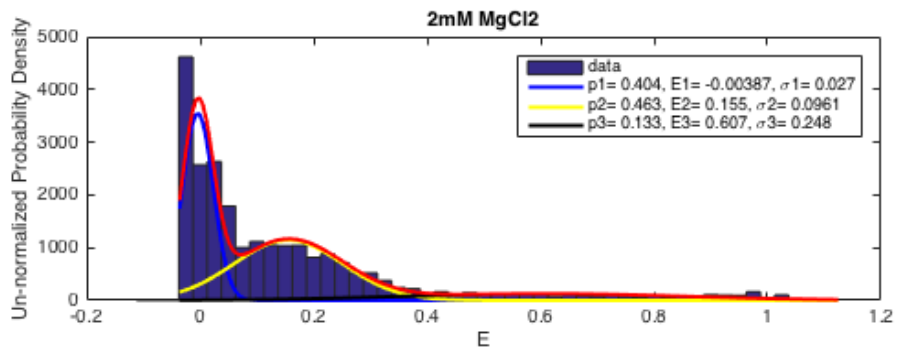
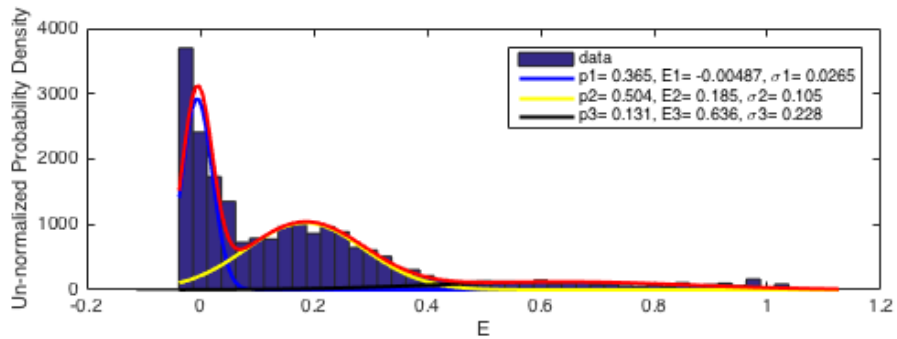
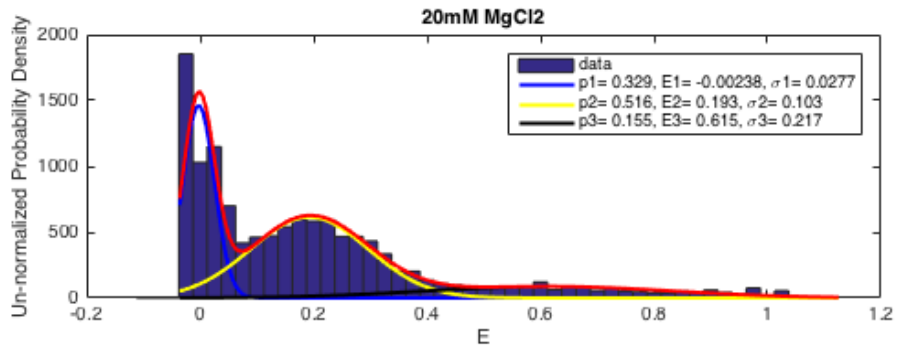
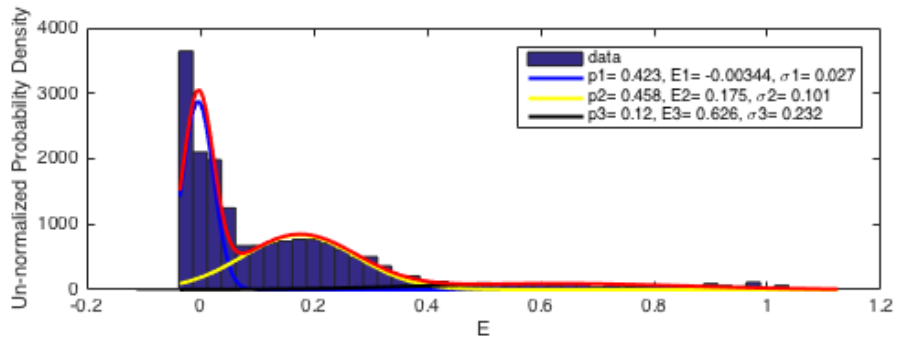
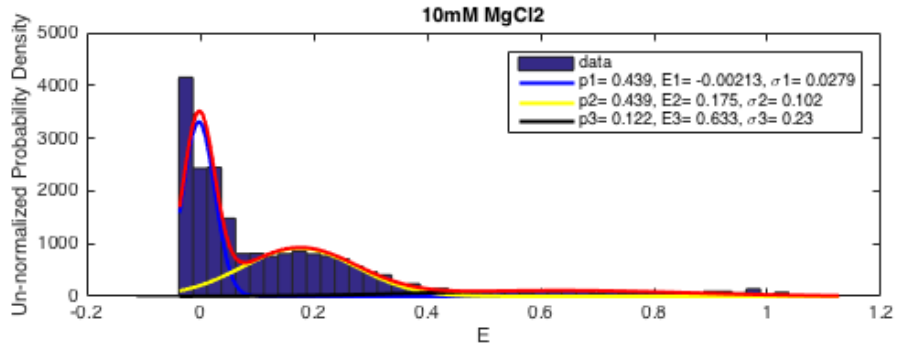


Figure S4 (below). FRET Histograms for H-J5/5a-H, D1-A (end labeled) in $MgCl_2$ solutions.







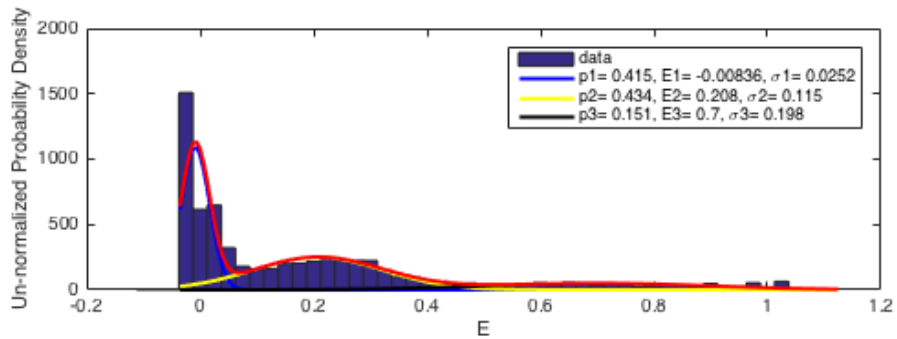
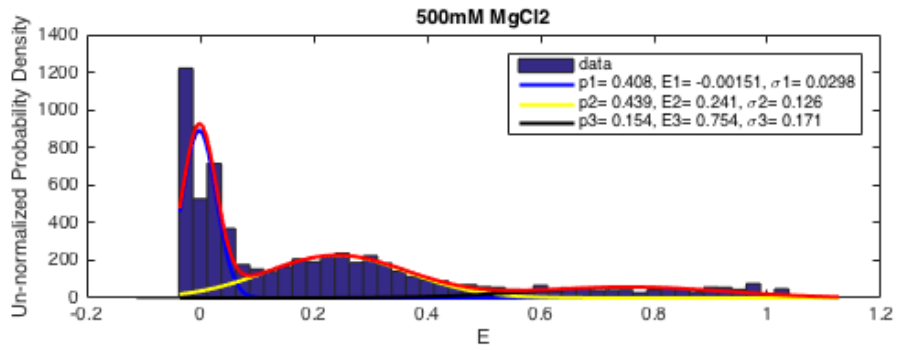
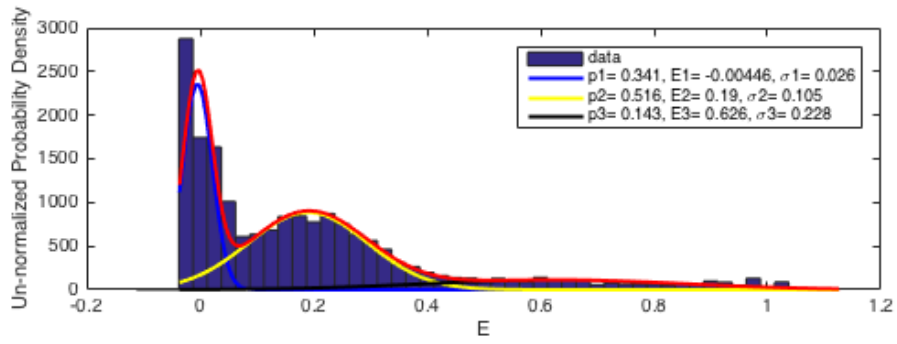
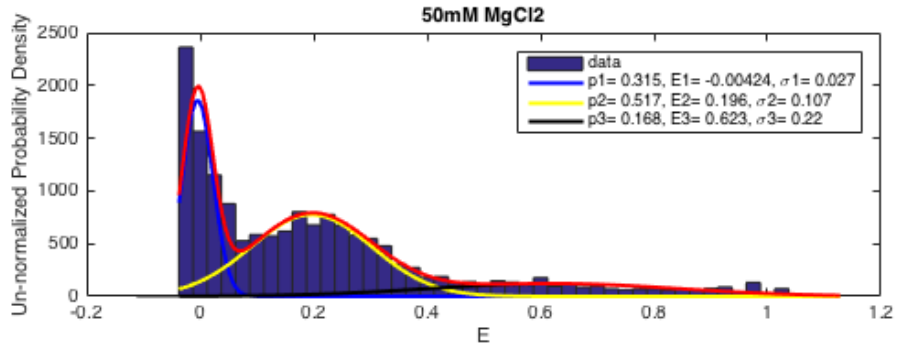
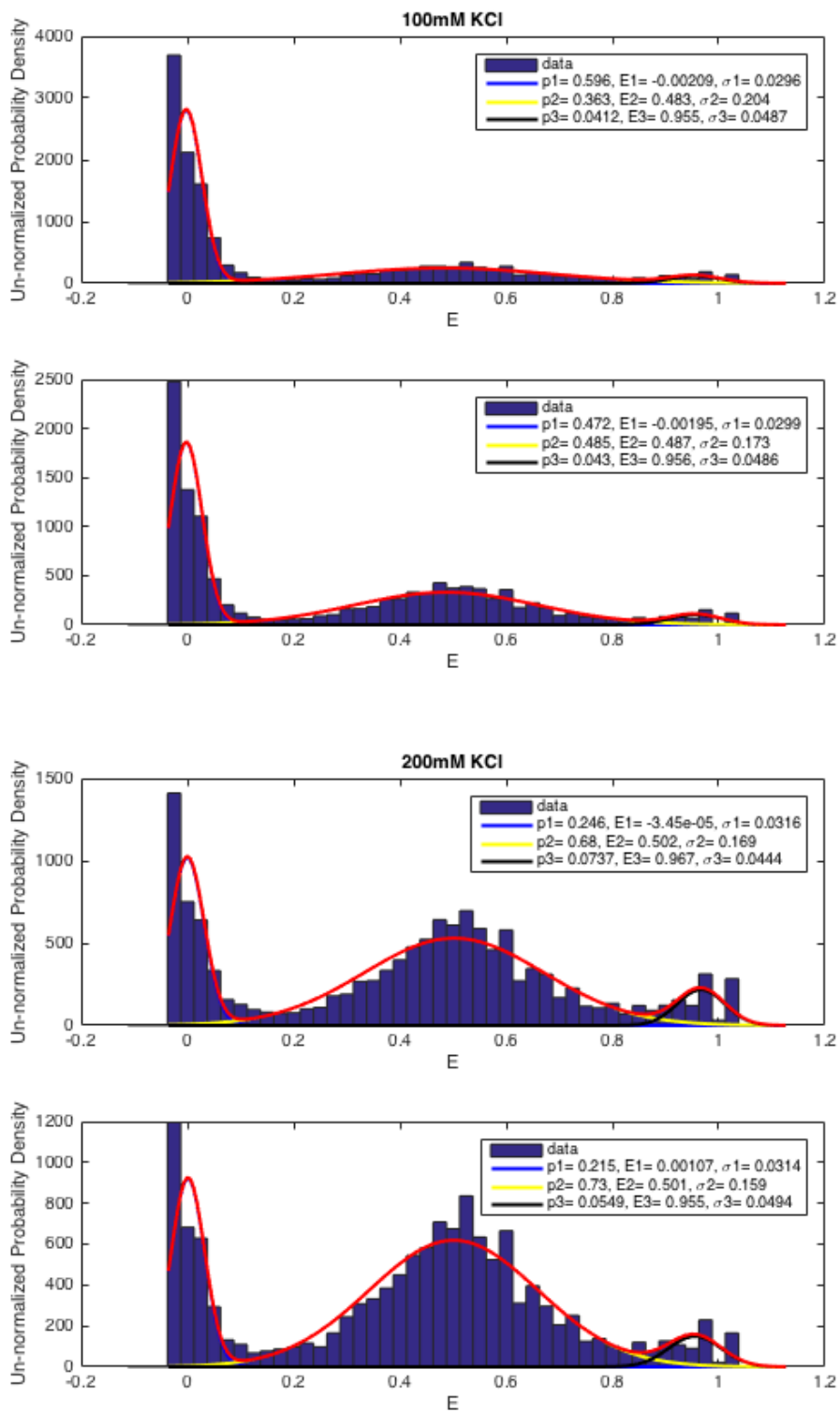
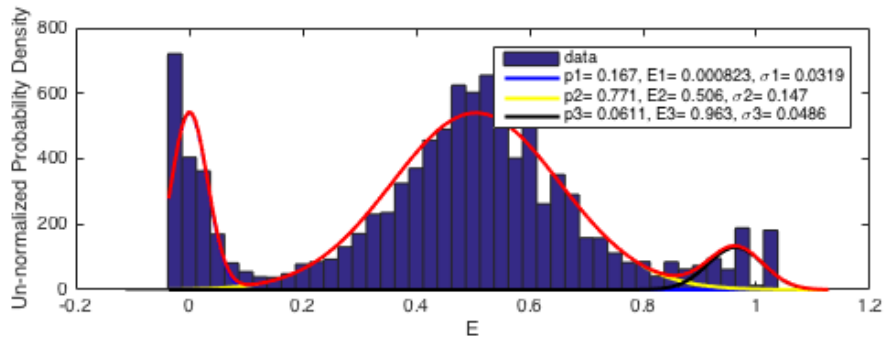
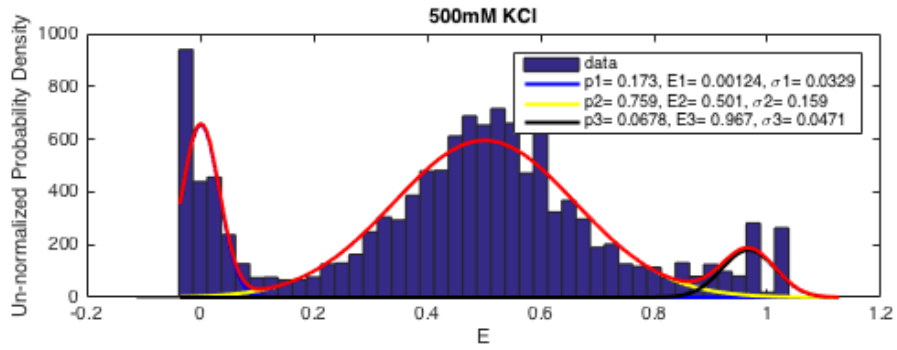
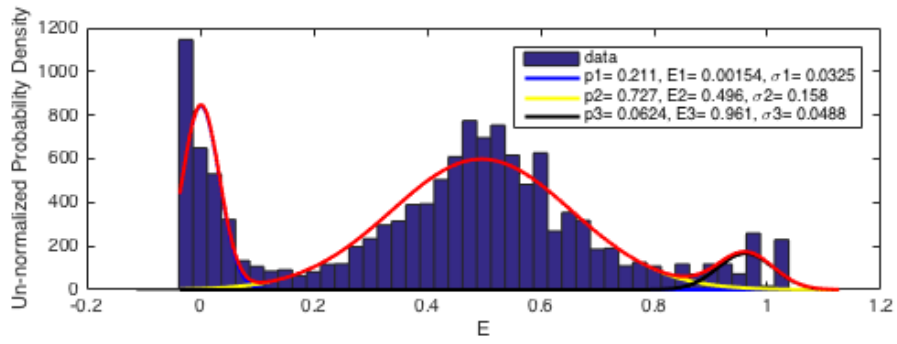
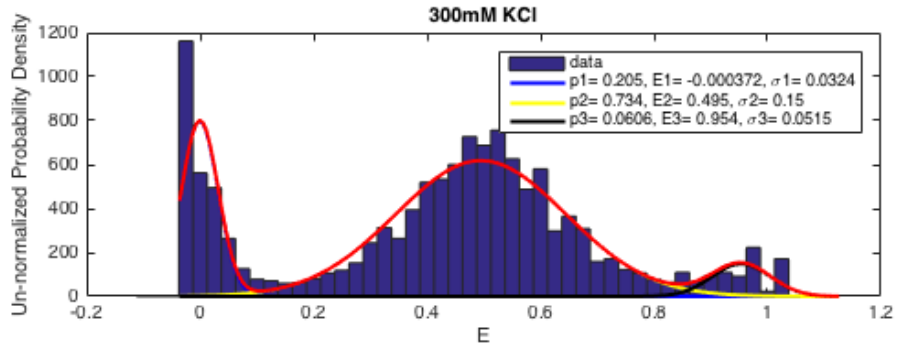


Figure S5 (below). FRET Histograms for H-JU₄U₅-H, D2-A (side labeled) in KCl solutions.





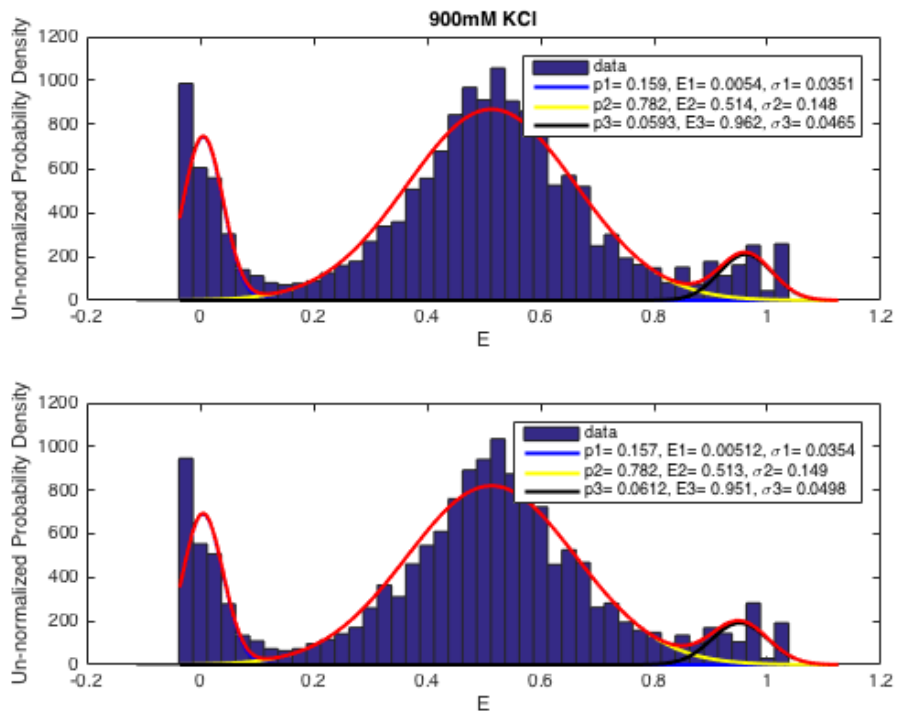
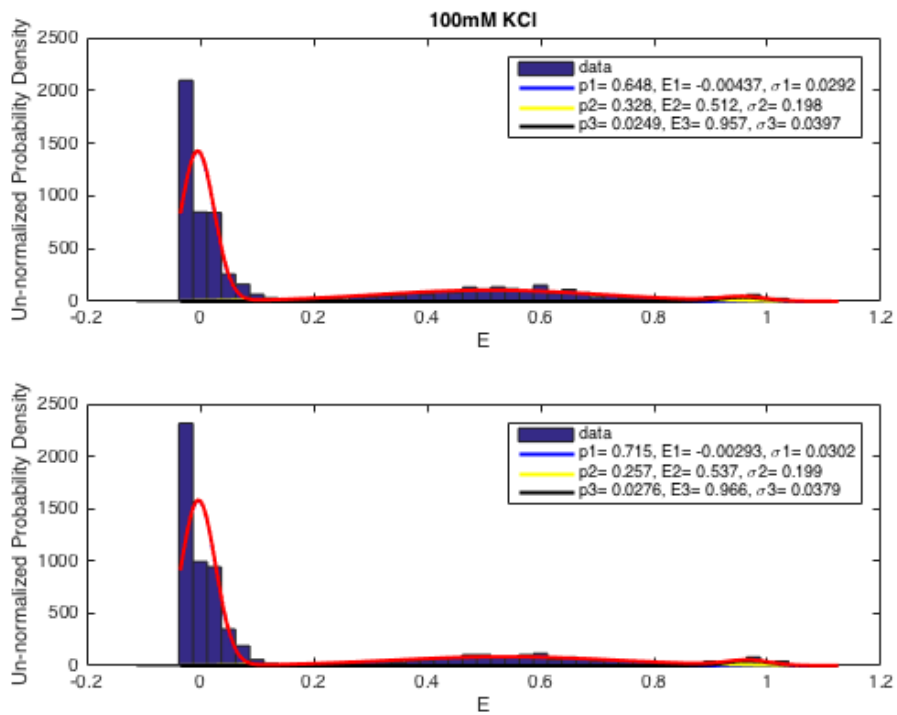
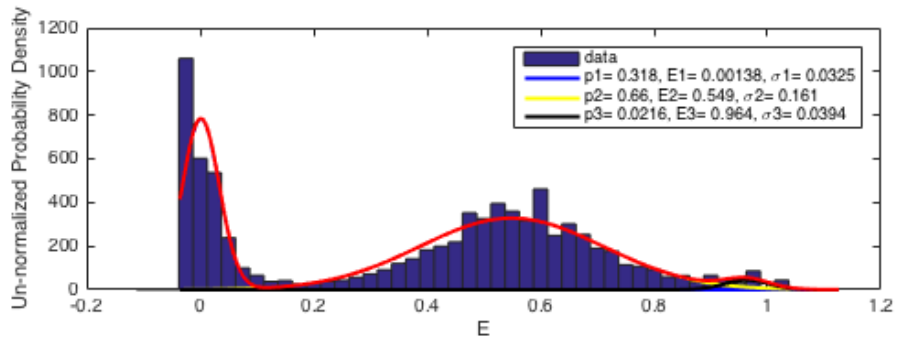
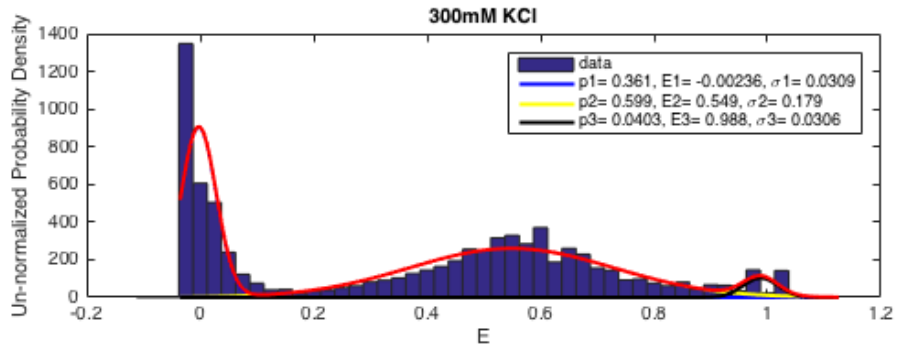
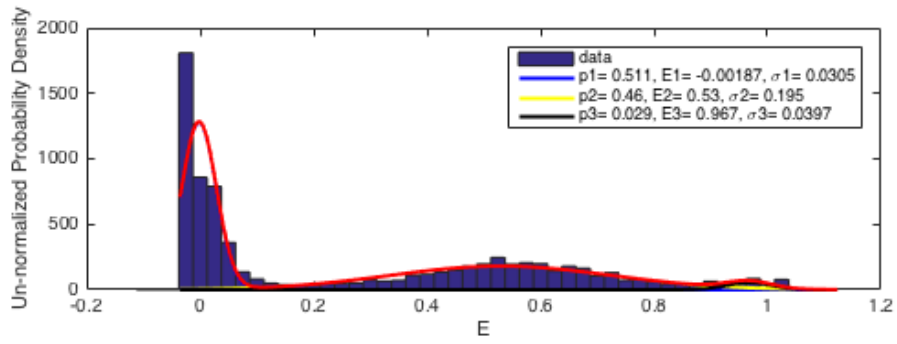
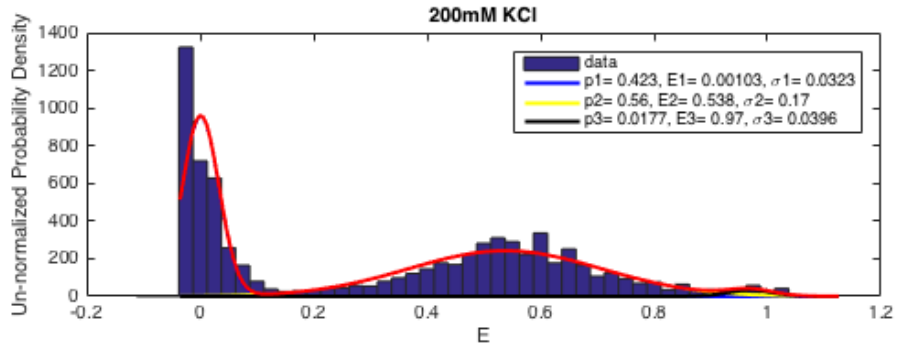


Figure S6 (below). FRET Histograms for H-J5/5a-H, D2-A (side labeled) in KCl solutions.





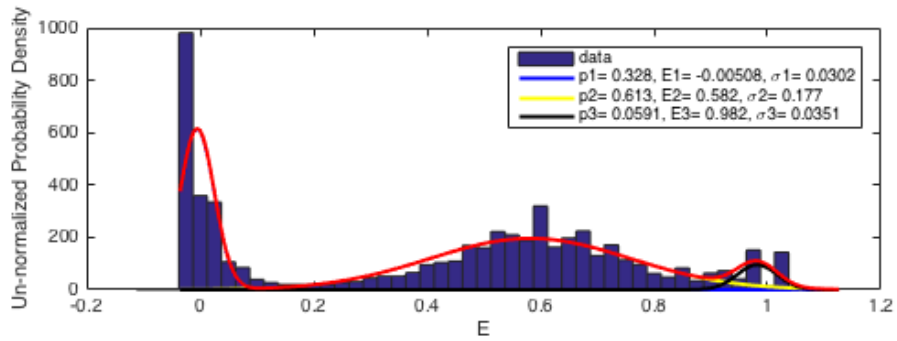
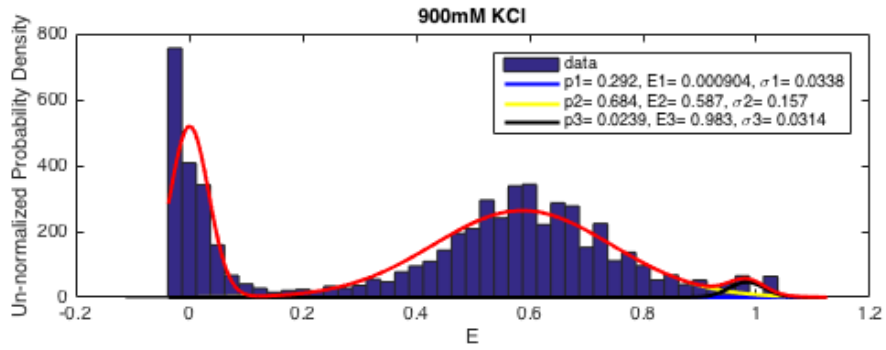
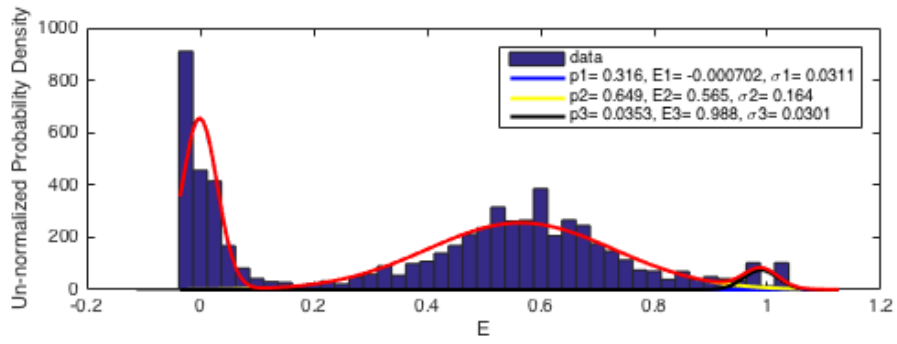
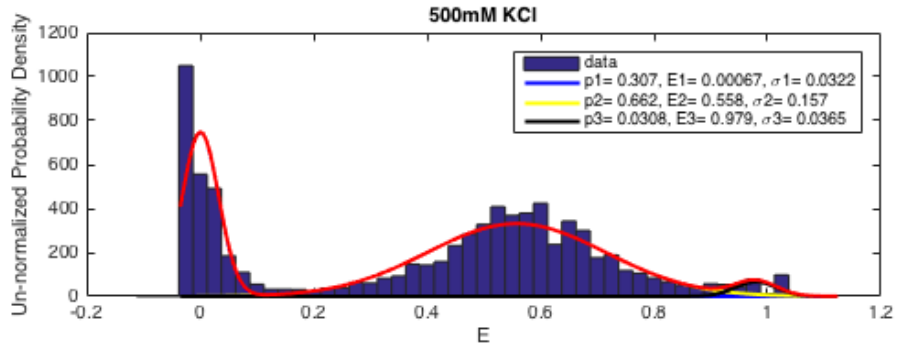
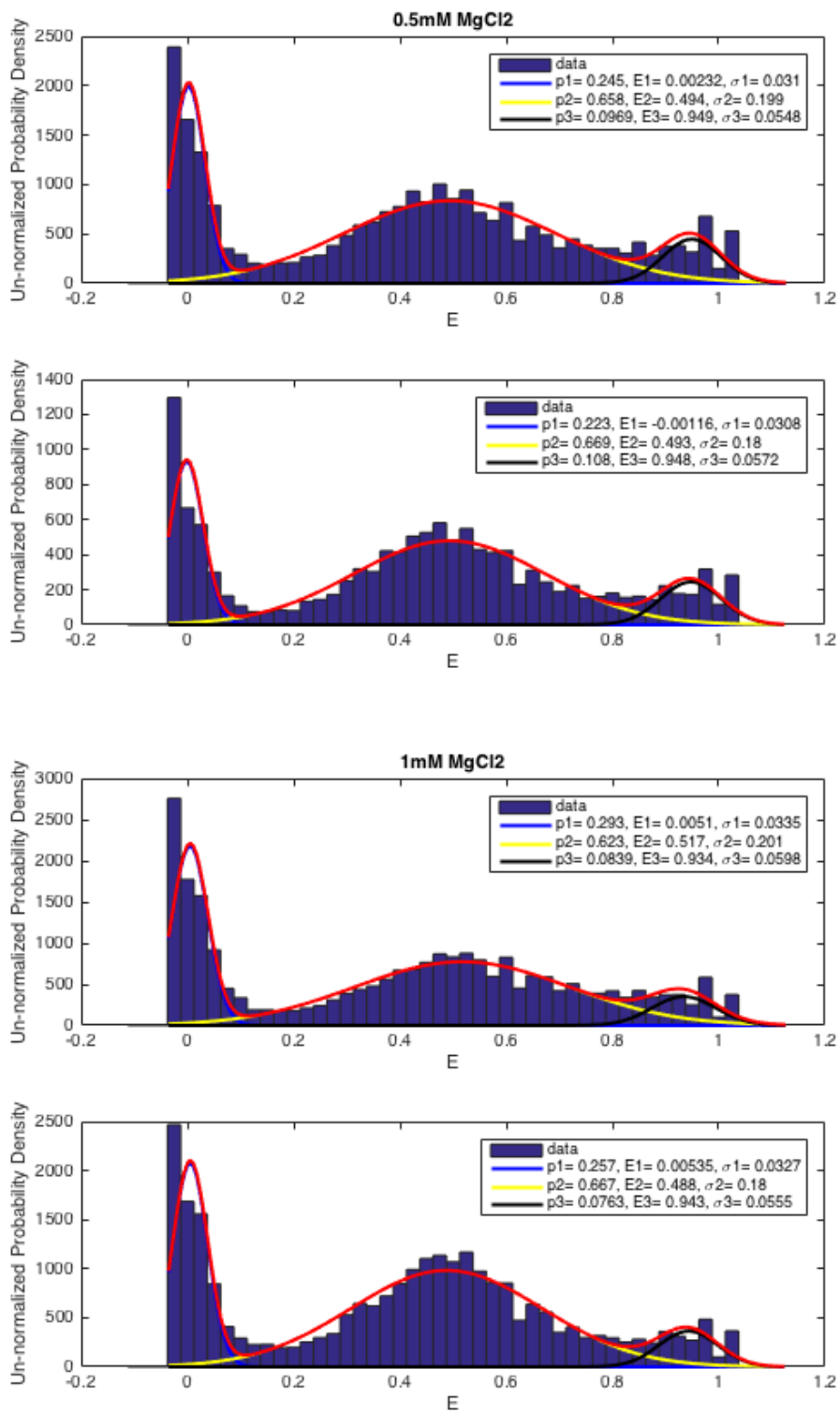
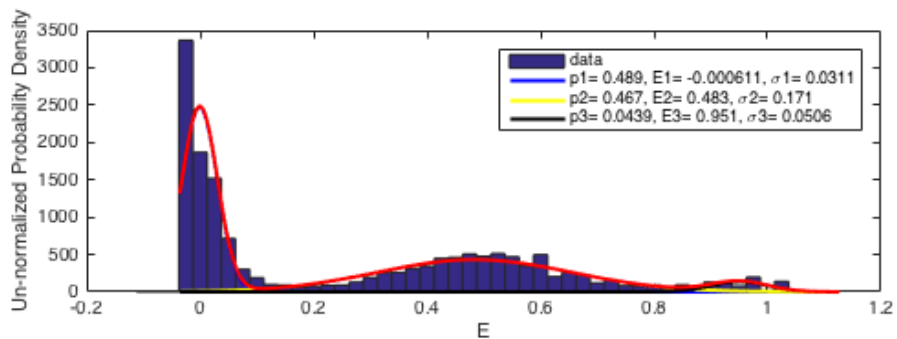
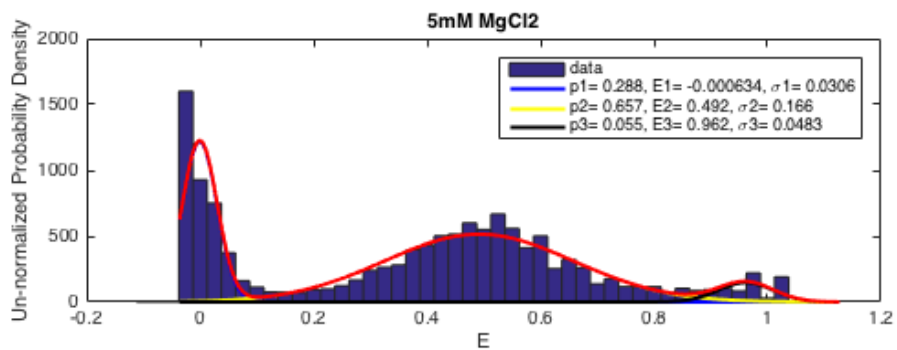
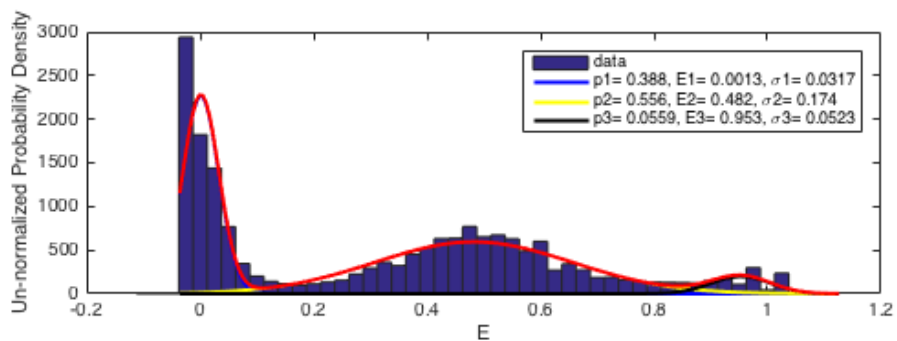
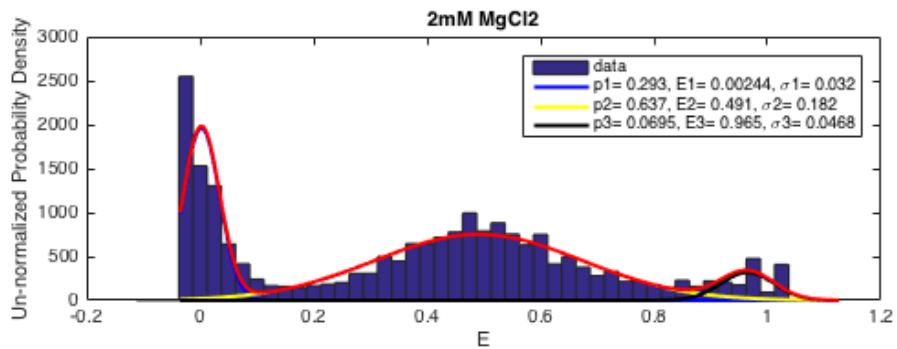
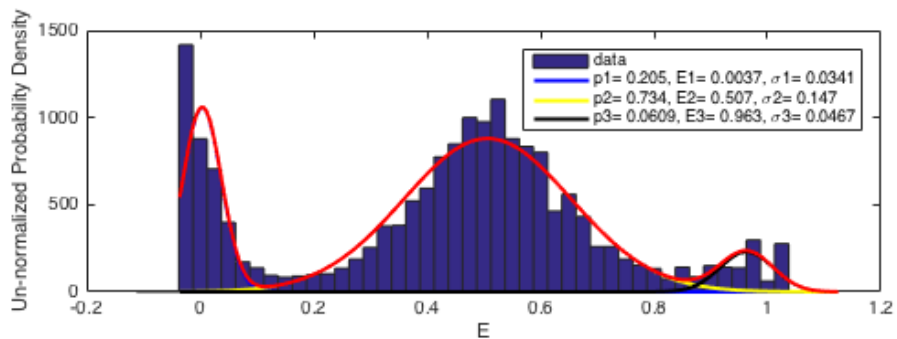
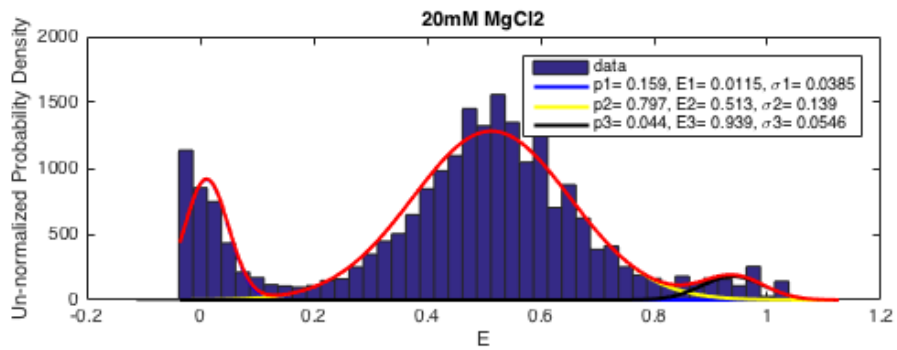
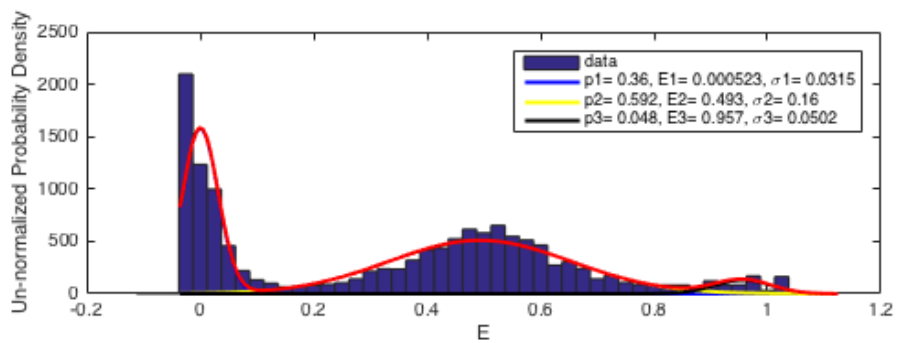
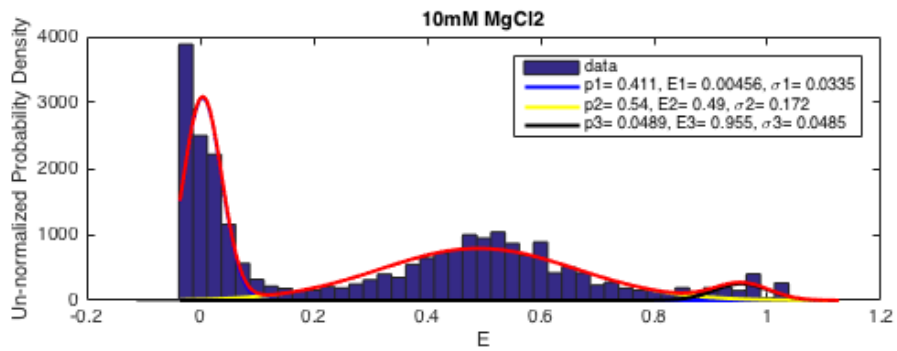


Figure S7 (below). FRET Histograms for H-JU₄U₅-H, D2-A (side labeled) in MgCl₂ solutions.







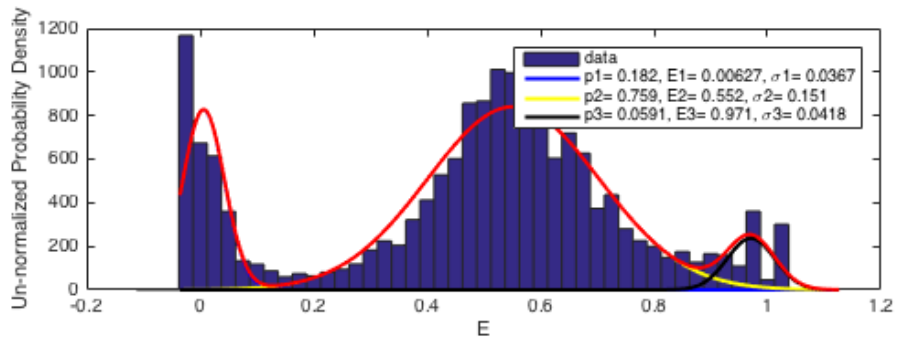
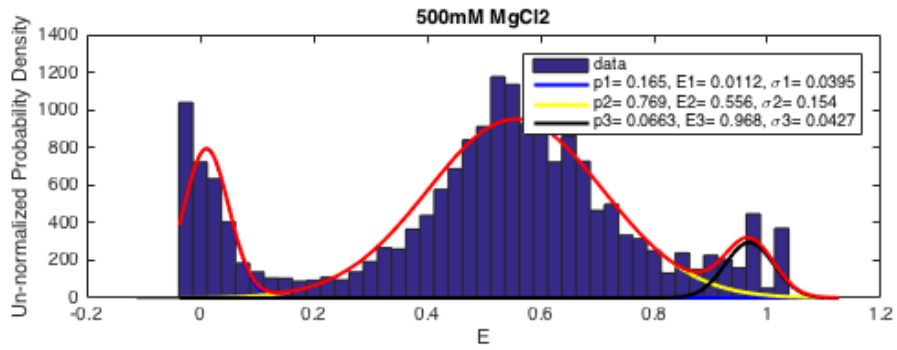
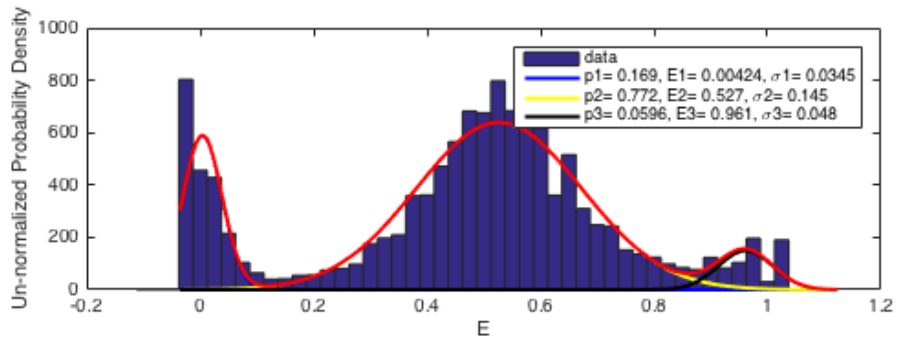
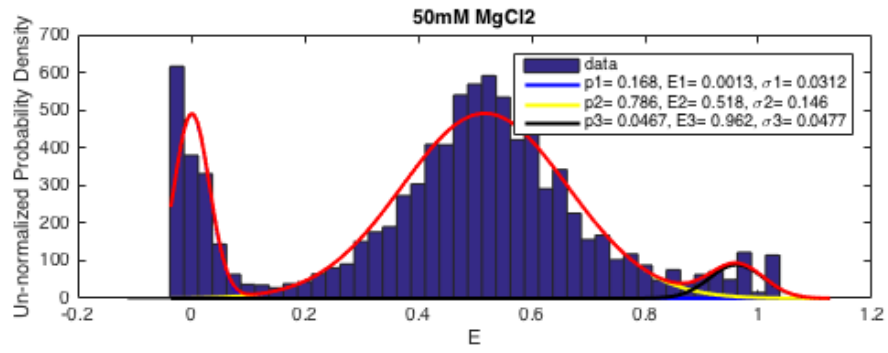
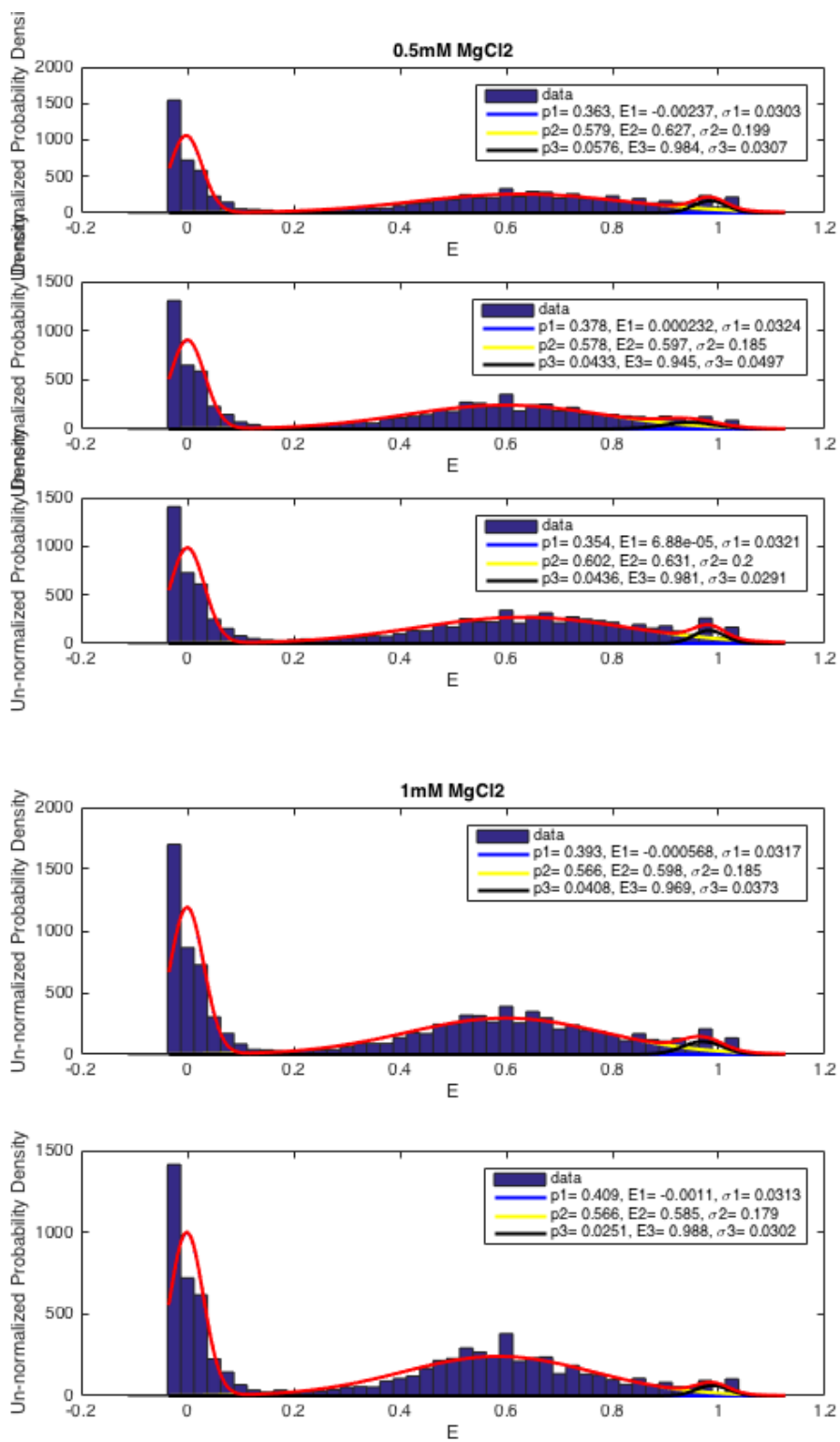
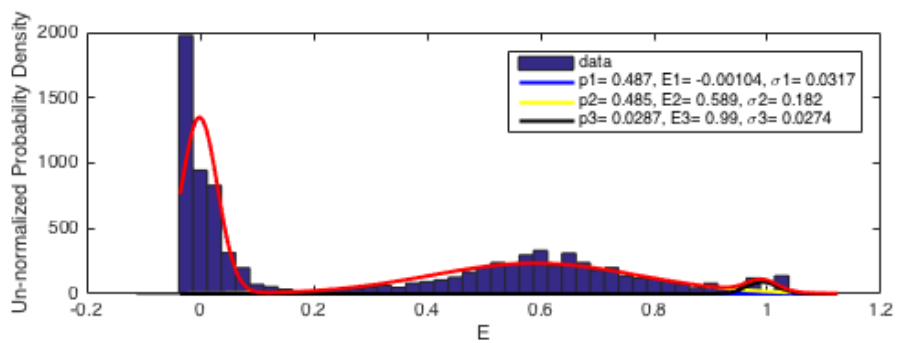
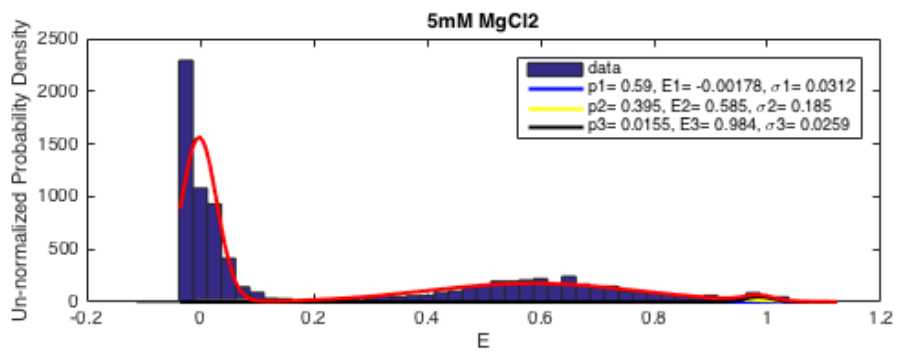
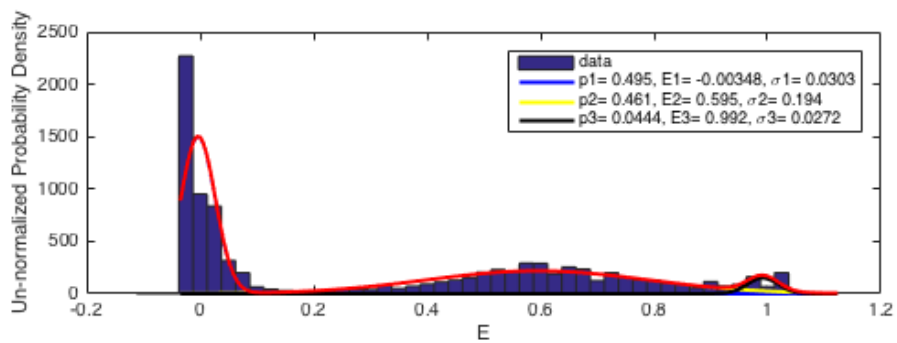
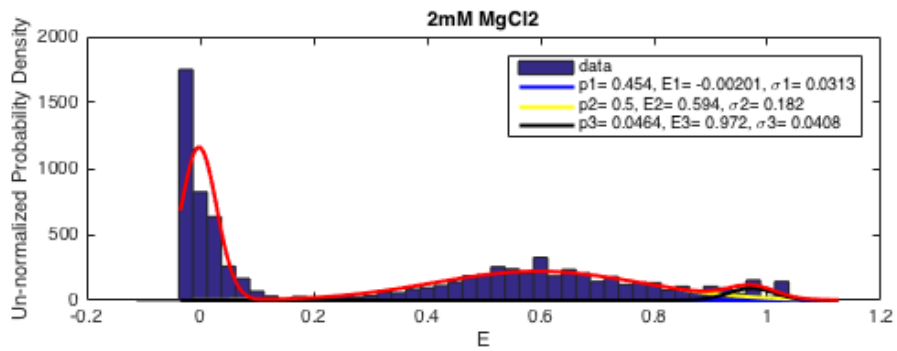
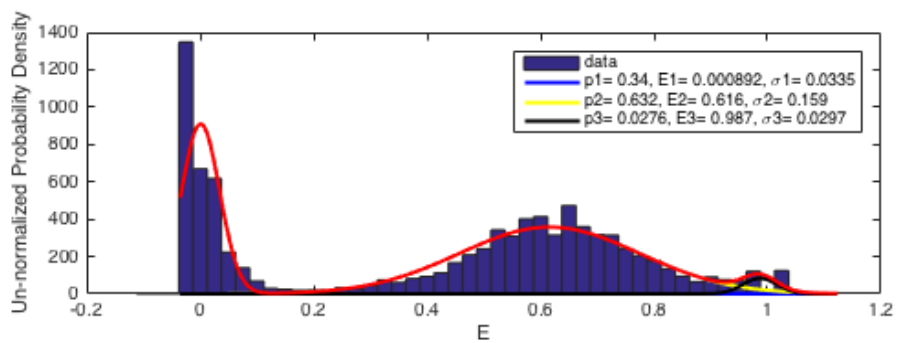
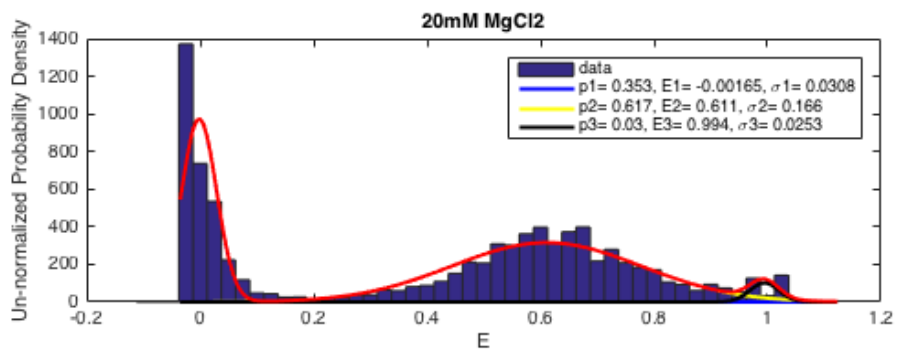
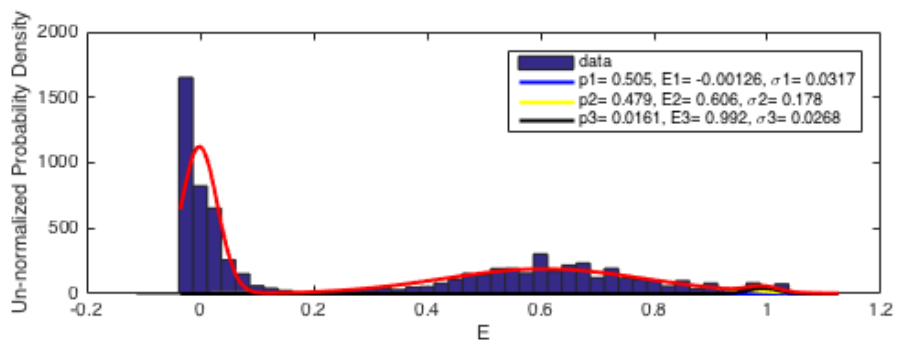
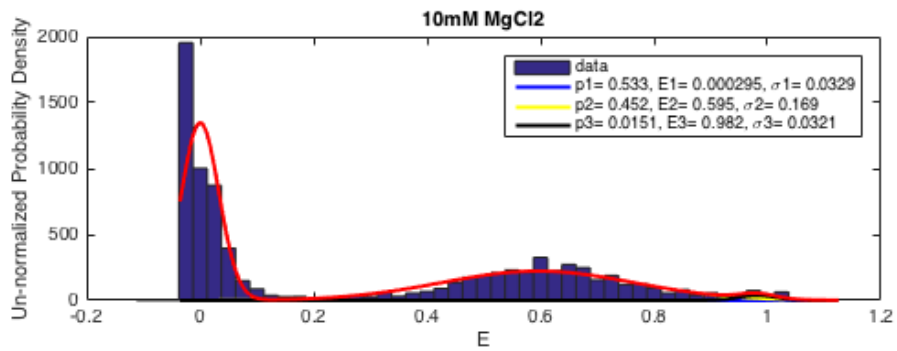


Figure S8 (below). FRET Histograms for H-J5/5a-H, D2-A (side labeled) in MgCl₂ solutions.







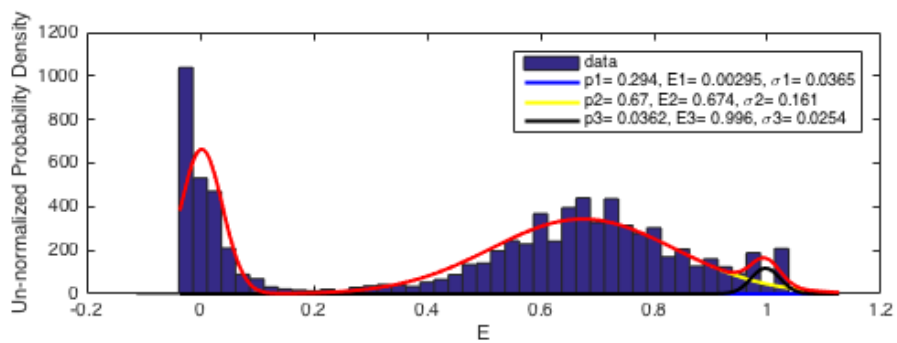
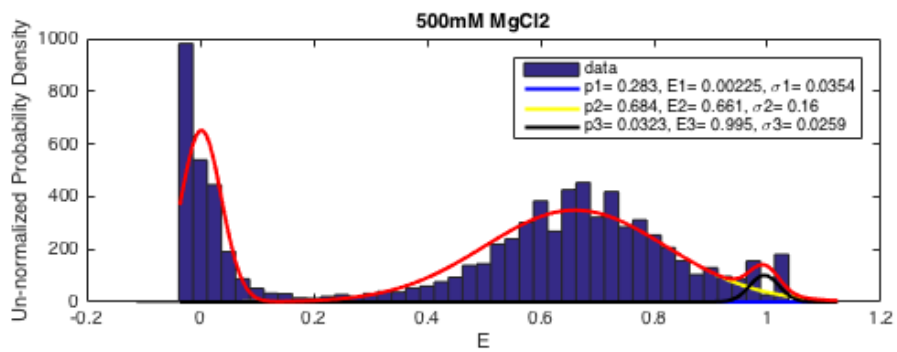
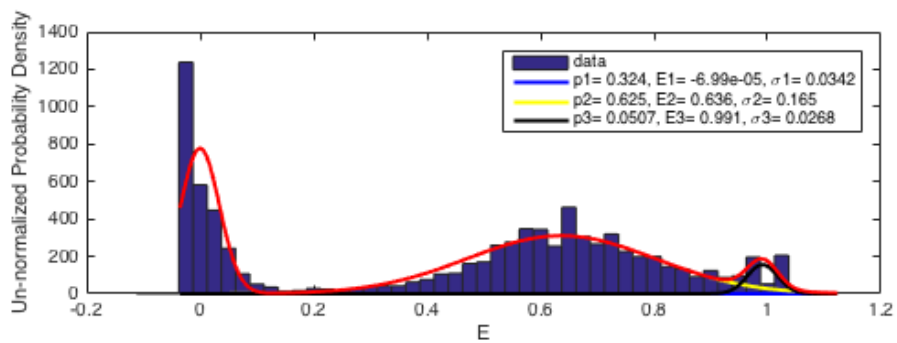
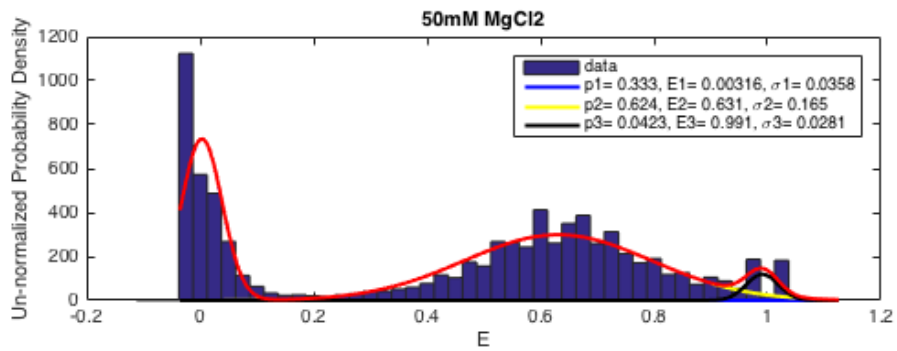
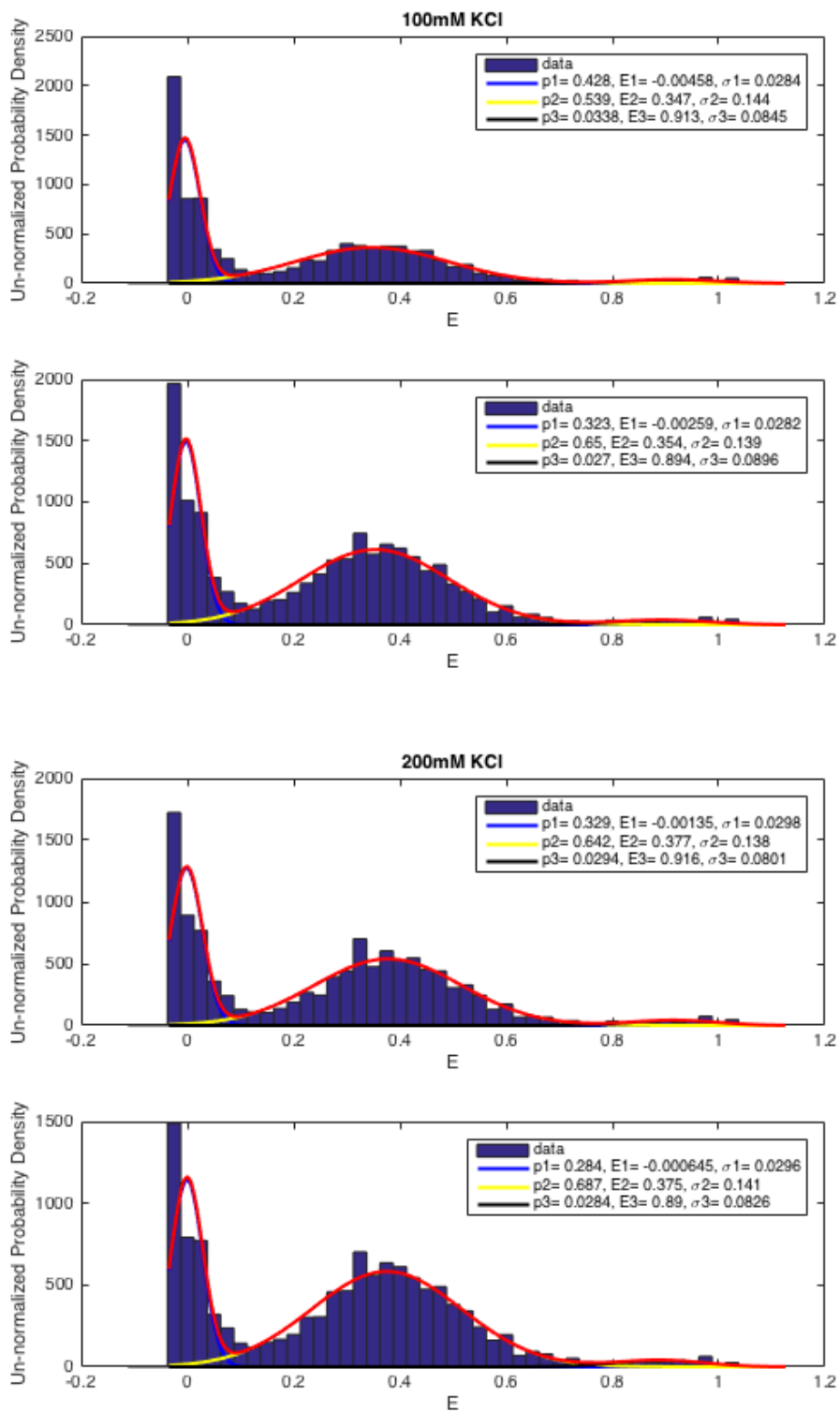
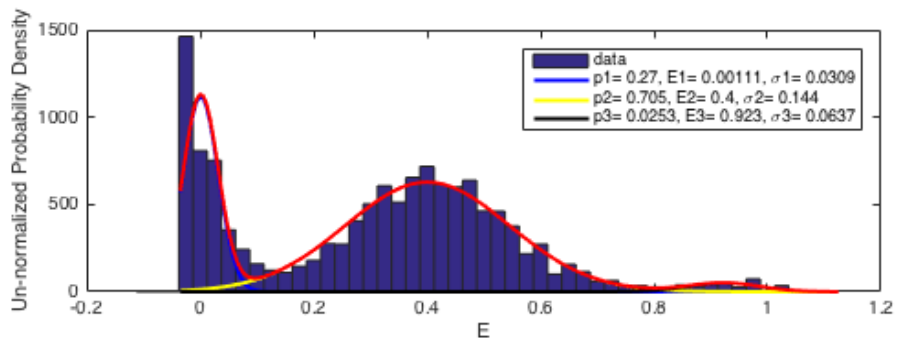
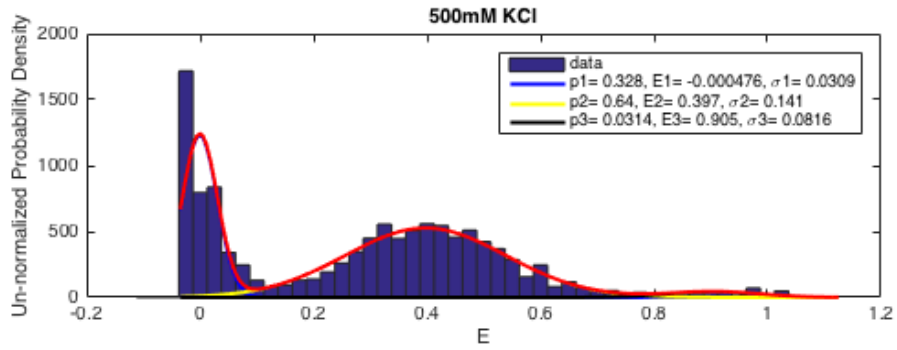
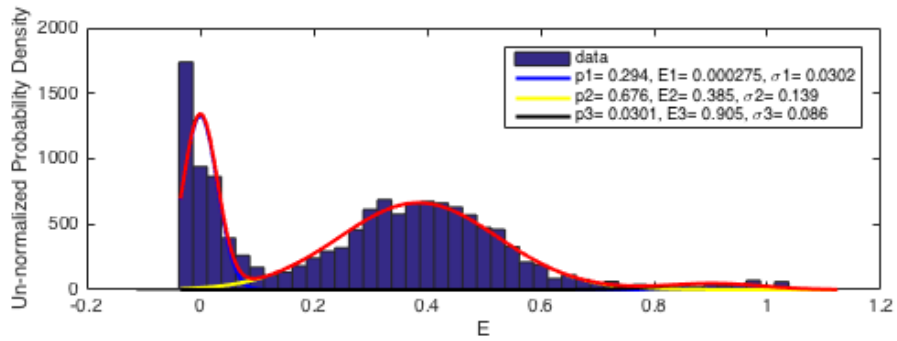
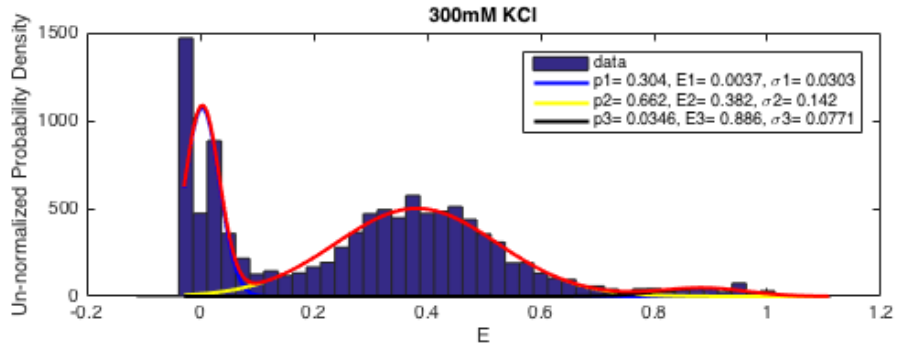


Figure S9 (below). FRET Histograms for H-JBP-H, D2-A (side labeled) in KCl solutions.





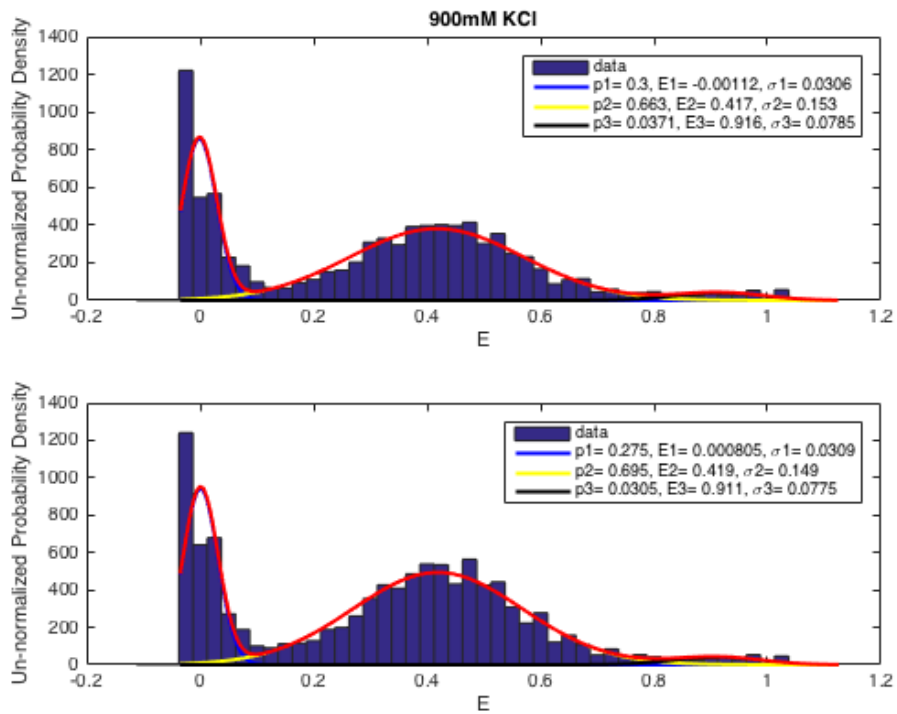
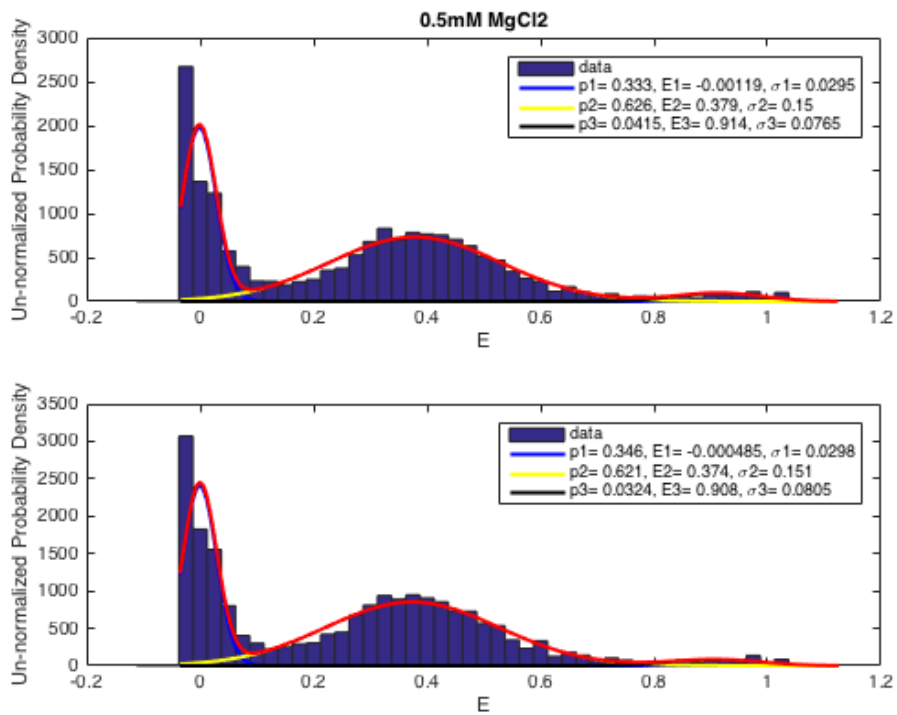
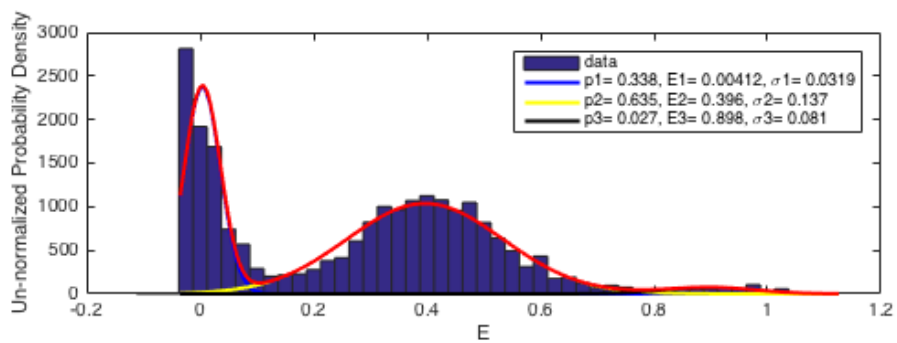
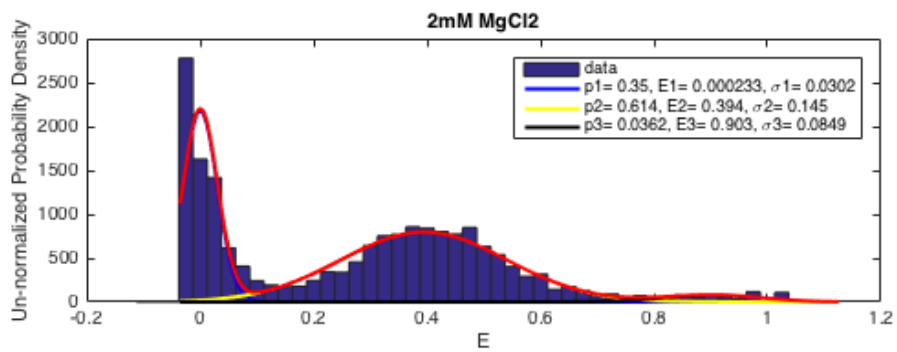
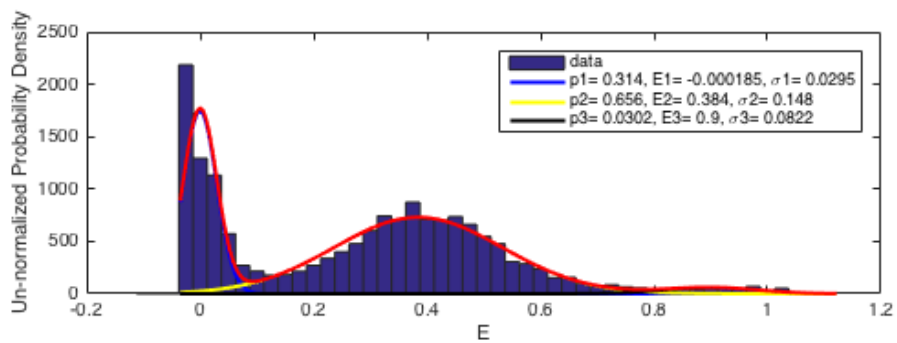
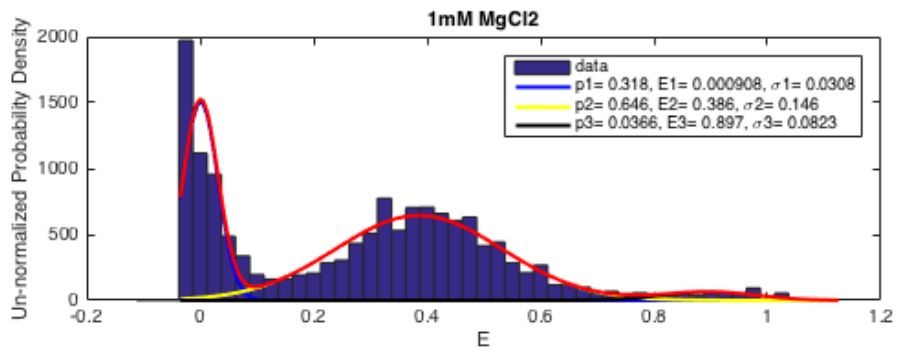
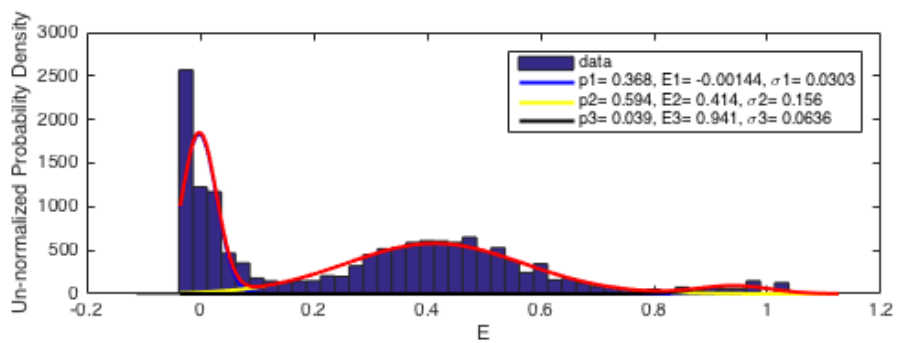
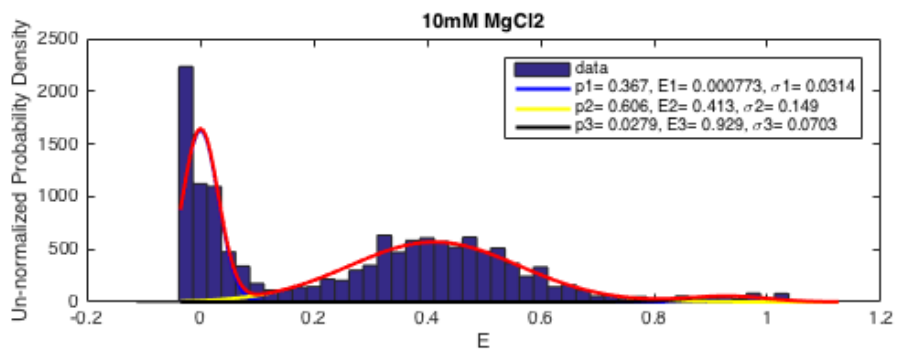
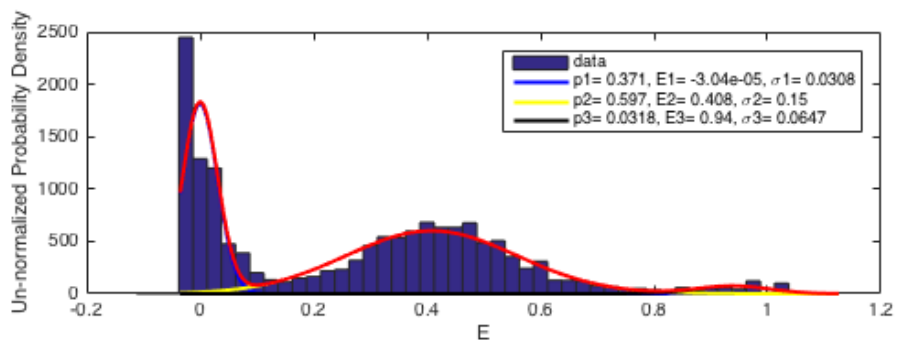
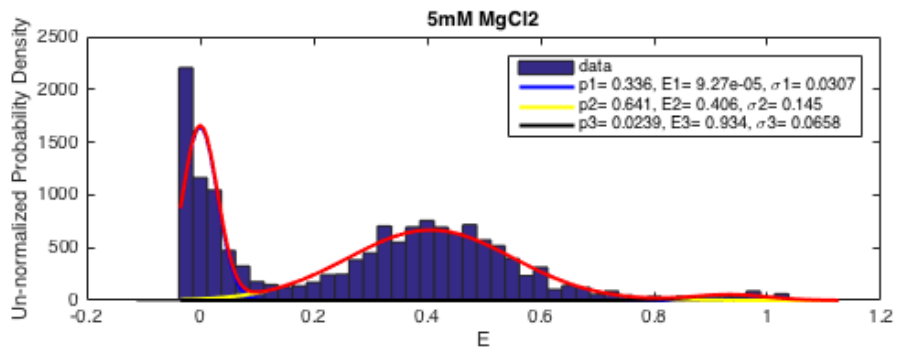
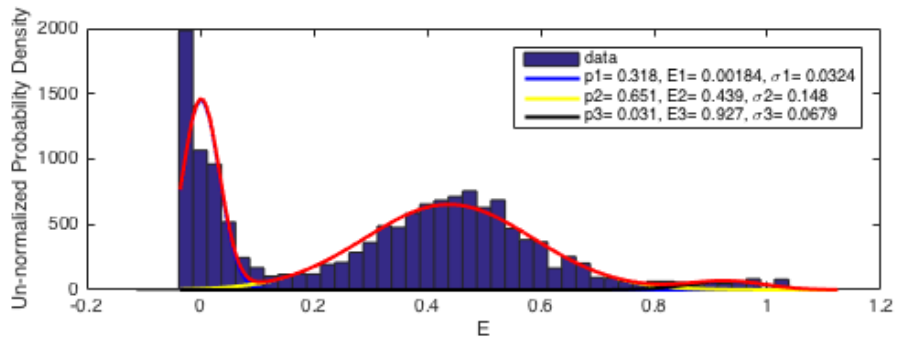
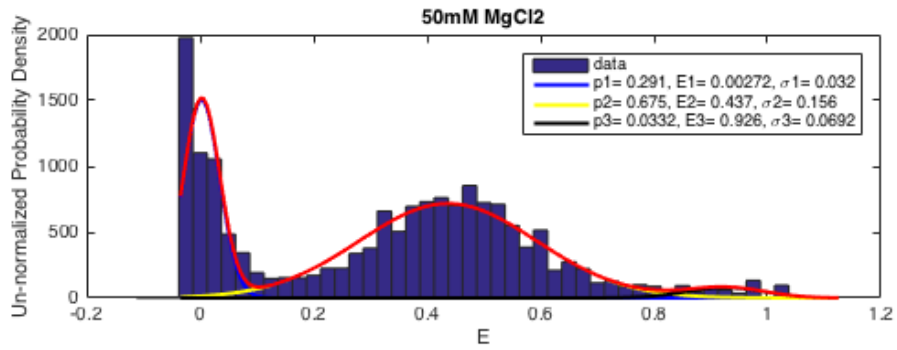
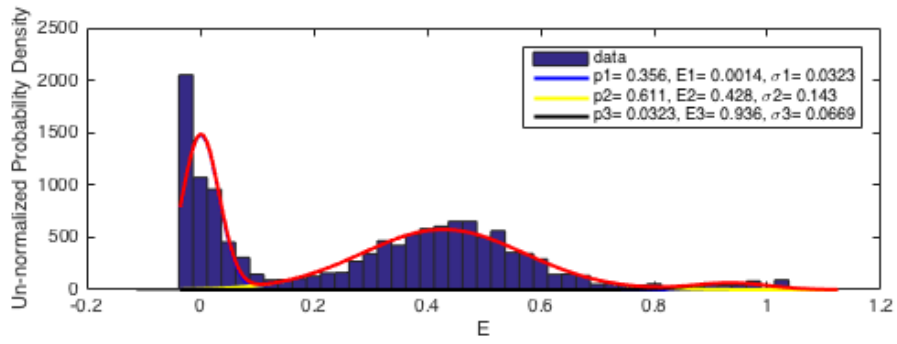
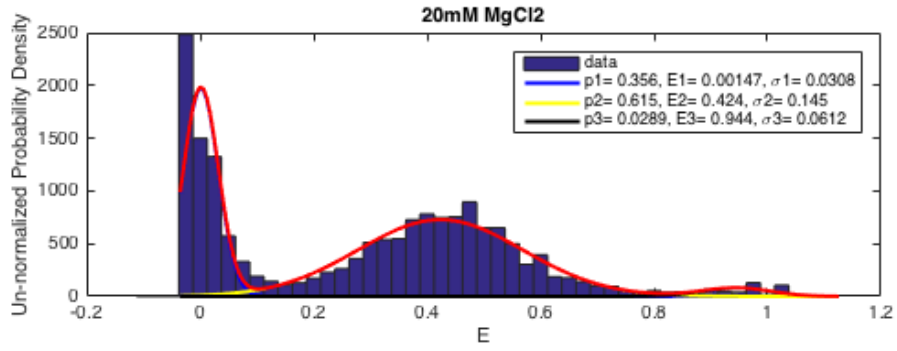


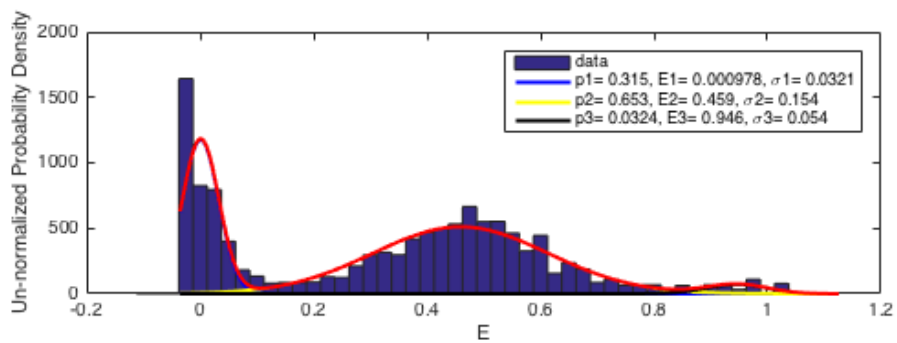
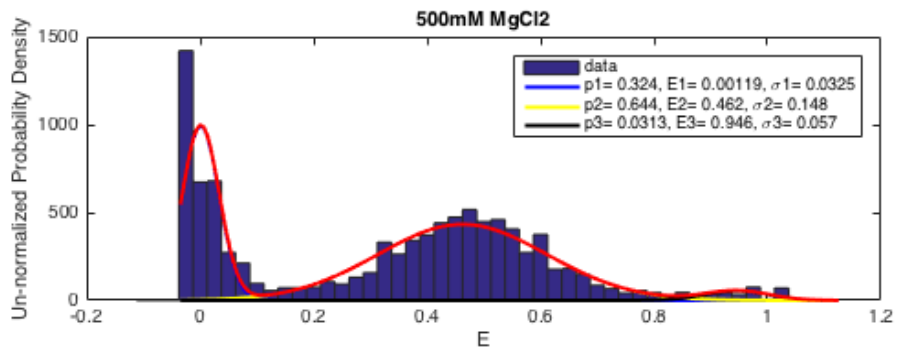
Figure S10 (below). FRET Histograms for H-JBP-H, D2-A (side labeled) in $MgCl_2$ solutions.











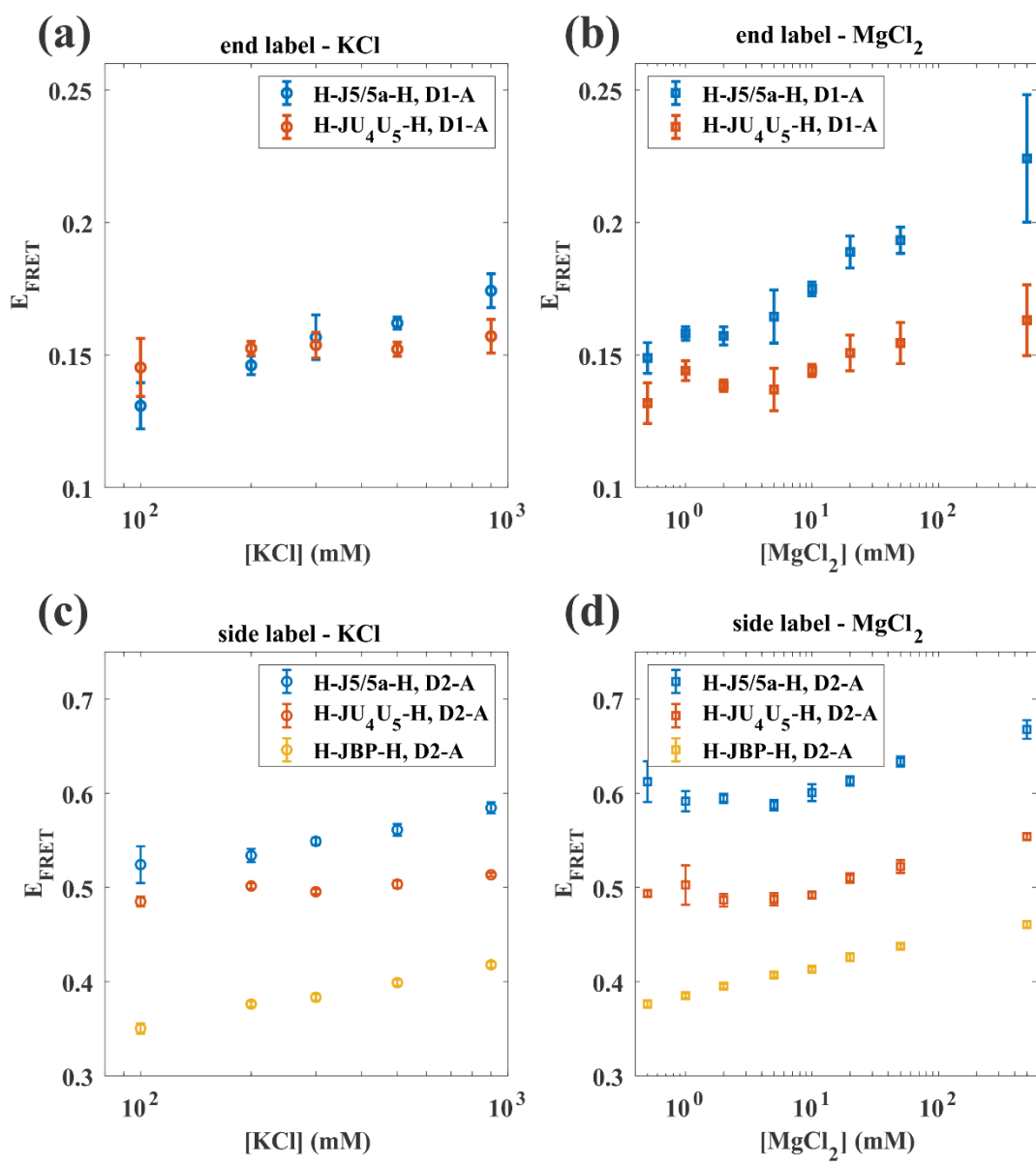


Figure S11. Measured effects on E_{FRET} of end-label donor dye position (D1-A dye pair) as a function of (a) KCl and (b) MgCl₂ for H-J5/5a-H and H-JU₄U₅-H isolated junction constructs and side-label donor dye position (D2-A dye pair) in (c) KCl and (d) MgCl₂ concentrations for H-J5/5a-H, H-JU₄U₅-H and H-JBP-H junction constructs.

Accessible Volume Simulations

All the sterically possible positions of fluorophores for the H-JBP-H RNA A-form duplex are calculated as a 3D probabilistic distribution by Accessible volume (AV) simulations¹. The software inputs are dye and linker parameters², atomic coordinates of the macromolecule to be labeled, and the attachment point of the dye linker on the molecule. The software computes the space which the dye can explore without steric clashes with the macromolecular surface. We used the Nucleic Acid Builder web server³ to build an A-form RNA helix with the same sequence as the H-JBP-H. Using the AV simulations, we calculated 3D probabilistic distributions for the donor and acceptor, P_D and P_A respectively, both of which are normalized.

$$\int P(\vec{r}) d\vec{r} = 1 \quad (1)$$

The average distance between the donor and acceptor is then

$$\langle R_{FRET} \rangle = \iint \|\vec{r}_D - \vec{r}_A\| P_D(\vec{r}_D) P_A(\vec{r}_A) d\vec{r}_D d\vec{r}_A \quad (2)$$

where \vec{r}_D and \vec{r}_A are donor and acceptor positions with respect to certain origin. The expected E_{FRET} can therefore be calculated.

$$\langle E_{FRET} \rangle = \frac{1}{1 + \left(\frac{\langle R_{FRET} \rangle}{R_0}\right)^6} \quad (3)$$

Note that we assume fast dye reorientation and relatively slow conformational dynamics.

AV simulation

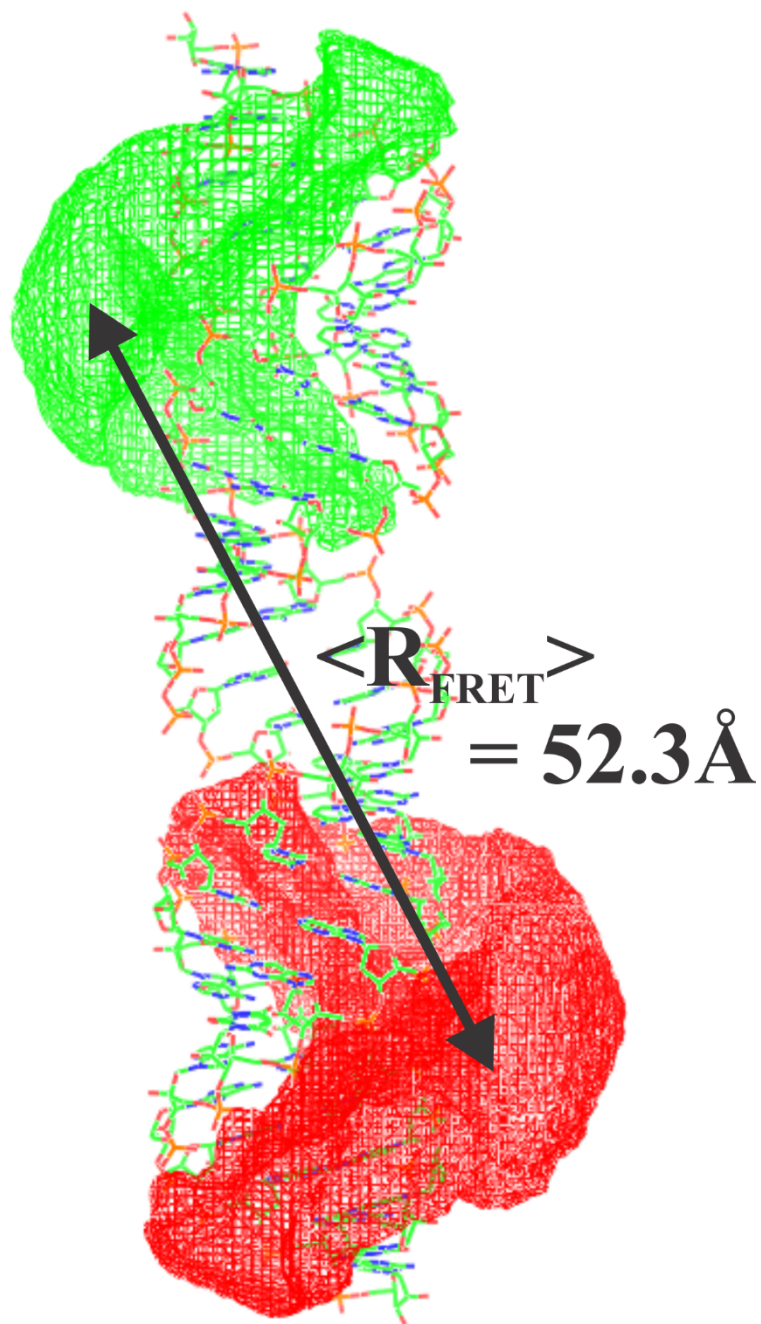


Figure S12. Representative accessible volumes of donor (green) and acceptor (red) dyes around the base-paired control RNA. The expected distance, $\langle R_{FRET} \rangle$ is 52.3 Å.

Comparison of smFRET Data Between DNA and RNA Duplex

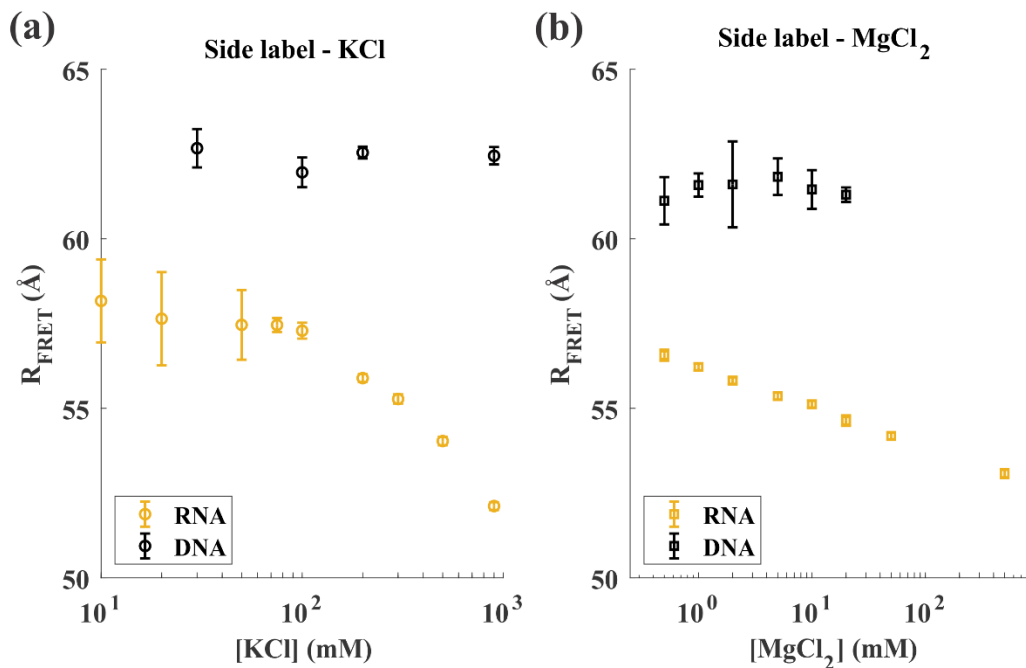


Figure S13. Comparison between RNA and DNA duplexes of the same length using the D2-A dye pair position in (a) KCl and (b) MgCl_2 solutions. The DNA B-form duplex remains stable throughout salt species and concentrations while RNA A-form duplex is twisted as ion strength increases.

REFERENCES

1. Muschielok A, Michaelis J. FRETnps Tools Documentation Starting FRETnpsTools. *Simulation*. 2008.
2. Sindbert S, Kalinin S, Nguyen H, et al. Accurate distance determination of nucleic acids via Förster resonance energy transfer: Implications of dye linker length and rigidity. *J Am Chem Soc*. 2011;133(8):2463-2480. doi:10.1021/ja105725e.
3. Macke TJ, Case DA. Modeling Unusual Nucleic Acid Structures BT - Molecular Modeling of Nucleic Acids. *Mol Model Nucleic Acids*. 2009;682:379-393. doi:10.1021/bk-1998-0682.ch024.